

University of Alabama in Huntsville

**LOUIS**

---

Theses

UAH Electronic Theses and Dissertations

---

2019

## **Kinematic analysis of gait in an aquatic treadmill using land-based motion capture cameras**

Shreyas Lakshmipuram Raghu

Follow this and additional works at: <https://louis.uah.edu/uah-theses>

---

### **Recommended Citation**

Lakshmipuram Raghu, Shreyas, "Kinematic analysis of gait in an aquatic treadmill using land-based motion capture cameras" (2019). *Theses*. 637.  
<https://louis.uah.edu/uah-theses/637>

This Thesis is brought to you for free and open access by the UAH Electronic Theses and Dissertations at LOUIS. It has been accepted for inclusion in Theses by an authorized administrator of LOUIS.

**KINEMATIC ANALYSIS OF GAIT IN AN AQUATIC TREADMILL USING  
LAND - BASED MOTION CAPTURE CAMERAS**

**by**

**SHREYAS LAKSHMIPURAM RAGHU**

**A THESIS**

**Submitted in partial fulfillment of the requirements  
for the degree of Master of Science in Engineering  
in  
The Department of Mechanical and Aerospace Engineering  
to  
The School of Graduate Studies  
of  
The University of Alabama in Huntsville**

**HUNTSVILLE, ALABAMA  
2019**

In presenting this thesis in partial fulfillment of the requirements for a master's degree from The University of Alabama in Huntsville, I agree that the Library of this University shall make it freely available for inspection. I further agree that permission for extensive copying for scholarly purposes may be granted by my advisor or, in his/her absence, by the Chair of the Department or the Dean of the School of Graduate Studies. It is also understood that due recognition shall be given to me and to The University of Alabama in Huntsville in any scholarly use which may be made of any material in this thesis.

*Shreyas L.R.*

Shreyas Lakshmipuram Raghu


07/15/19

(Date)

## THESIS APPROVAL FORM

Submitted by Shreyas Lakshmpuram Raghu in partial fulfillment of the requirements for the degree of Master of Science in Engineering in Aerospace Systems Engineering and accepted on behalf of the Faculty of the School of Graduate Studies by the thesis committee.

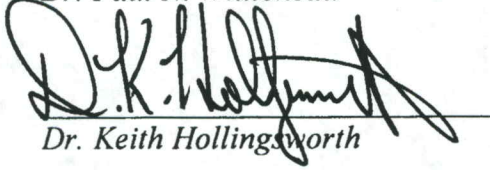
We, the undersigned members of the Graduate Faculty of The University of Alabama in Huntsville, certify that we have advised and/or supervised the candidate of the work described in this thesis. We further certify that we have reviewed the thesis manuscript and approve it in partial fulfillment of the requirements for the degree of Master of Science in Engineering in Aerospace Systems Engineering.

  
\_\_\_\_\_  
Dr. Chang-kwon Kang      7/15/19      Committee Chair  
(Date)


  
\_\_\_\_\_  
Dr. D. Brian Landrum      8/5/19  
(Date)

  
\_\_\_\_\_  
Dr. Ryan T. Conners      7/22/19  
(Date)

  
\_\_\_\_\_  
Dr. Paul N. Whitehead      7/31/19  
(Date)

  
\_\_\_\_\_  
Dr. Keith Hollingsworth      8/6/19      Department Chair  
(Date)

  
\_\_\_\_\_  
Dr. Shankar Mahalingam      8/9/19      College Dean  
(Date)  
For Shankar Mahalingam

  
\_\_\_\_\_  
Dr. David Berkowitz      8/9/19      Graduate Dean  
(Date)



## ABSTRACT

School of Graduate Studies  
The University of Alabama in Huntsville

Degree Masters of Science College/Dept. Engineering/Mechanical and  
in Engineering Aerospace Engineering

Name of Candidate: Shreyas Lakshmipuram Raghu

Title: Kinematic analysis of gait in an aquatic treadmill using land based motion capture cameras

While the capabilities of land-based motion capture systems in biomechanics applications have been previously reported, the possibility of using external optical motion tracking systems to reconstruct markers submerged inside an aquatic environment has been underexplored. The use of optical motion tracking system can especially be suited for applications within constrained aquatic environments such as an underwater treadmill that restrict the ability to use conventional aquatic motion capture systems. This study assesses the ability of a land-based motion capture system, arranged externally, to track a set of retro-reflective markers inside an aquatic environment. First, customized reflective marker was developed such that the reflective properties could be sustained underwater. The motion capture cameras were then tested for accuracy in marker reconstruction under water. Finally, experiments were conducted where healthy individuals walked in an aquatic treadmill at different speeds for kinematic assessments. This helps in quantifying the benefits of walking in the presence of water (condition 2), as opposed to conventional dry-land treadmill walking for rehabilitation (condition 1). The results suggest that there is no

significant influence of the presence of water on the accuracy outcomes (trueness and precision) of the marker center distances when markers were made of SOLAS grade reflective tape. Further, the kinematic analysis revealed greater peak knee and ankle angles with the gait speed, whereas the time taken to achieve these peaks reduced in both conditions. There is a statistically significant influence of the medium in time measures. In contrast, the angle measures, knee and ankle angles, were not seen to be statistically significantly different.

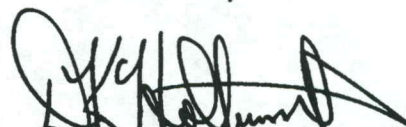
Abstract Approval: Committee Chair



---

*Dr. Chang-kwon Kang*

Department Chair



---

*Dr. Keith Hollingsworth*

Graduate Dean



---

*Dr. David Berkowitz*

## ACKNOWLEDGEMENTS

First, I would like to express my sincere gratitude to my committee chair and advisor, Dr. Chang-kwon Kang. He has guided me through all dimensions of my research and been an outstanding mentor throughout all stages of work. Also, I like to express my gratitude equally to my advisor Dr. Ryan T. Conners for his valuable inputs and guidance on various aspects of this research.

I sincerely appreciate my committee members Dr. D. Brian Landrum and Dr. Paul N. Whitehead for all their valuable advice and suggestions in adding more value to this thesis.

I like to thank UAH staff and faculty members Euan Holton, Zeke Aguilera and Claudia Meyering (retired) for their assistance. I like to extend my gratitude to my fellow graduate students, Madhu Sridhar, Jeremy Pohly and Jesse McCain. I would also like to extend my appreciation to alumni, Dr. Deepa Kodali and Kabilan Nenduchezian. Particularly, I like to thank Madhu from whom I learnt a lot about working with motion capture systems.

I want to thank my parents, brother and grandpa for all their support, sacrifice and hardships. I want to express my gratitude to all my friends for their moral support and encouragement.



## TABLE OF CONTENTS

LIST OF FIGURES.....	ix
LIST OF TABLES.....	xi
LIST OF SYMBOLS AND ABBREVIATIONS.....	xii
1. INTRODUCTION .....	1
1.1 Background and Motivation.....	1
1.2 Research Objectives .....	2
1.3 Thesis Outline .....	4
1.4 Content Disclaimer.....	4
1.5 Human Subjects Research.....	5
2. LITERATURE REVIEW .....	6
2.1 Motion Capture and Human Locomotion .....	6
2.2 Analysis of Human Locomotion .....	8
2.3 Human Locomotion in Water and Aquatic Rehabilitation.....	9
3. MATERIALS AND METHODS.....	14
3.1 Accuracy Analysis.....	14
3.1.1 Cameras, Markers, and Template.....	14
3.1.2 Calibration, Setup, and Processing.....	15
3.1.3 Procedure.....	17

3.1.4	Method of Analysis .....	18
3.2	Kinematic Analysis .....	20
3.2.1	Participants .....	20
3.2.2	Cameras, Calibration, Setup and Processing.....	21
3.2.3	Kinematic and Statistical Analysis.....	23
4.	RESULTS AND DISCUSSION .....	28
4.1	Accuracy Analysis.....	28
4.1.1	Calibration: Marker Distance Outcomes.....	28
4.1.2	Accuracy Outcomes .....	29
4.2	Kinematic Analysis .....	31
4.2.1	Influence of the Speed of the Treadmill.....	31
4.2.2	Air versus Water Conditions .....	35
4.3	Effect of Viscous Drag and Added Mass Forces .....	40
5.	CONCLUSION AND FUTURE SCOPE .....	49
5.1	Recommendation for Future Research.....	51
5.2	Novel Contributions .....	52
6.	APPENDIX A.....	54
7.	APPENDIX B .....	59
8.	REFERENCES .....	63

## LIST OF FIGURES

Figure	Page
<b>Figure 2-1:</b> Classification of important motion capture methods. ....	7
<b>Figure 2-2:</b> Anatomical planes of the body [27]. ....	8
<b>Figure 2-3:</b> Illustration of a complete gait cycle and gait events. ....	9
<b>Figure 3-1:</b> Marker creation and reference template for static measurements. (A) SOLAS reflective tape cut into petals of equal sizes wound around a spherical marker (length, $l = \pi d_m = 43.98$ mm). (B) Static reference template used for analysis with measured distances between marker centers; ( $d_1$ : Distance between markers $M_r$ and $M_1$ ; $d_2$ : Distance between markers $M_r$ and $M_2$ ; $d_3$ : Distance between markers $M_r$ and $M_3$ ). ....	15
<b>Figure 3-2:</b> Vicon wand with five precisely spaced markers. ....	16
<b>Figure 3-3:</b> Experimental setup and test schematic. (A) Cameras C1-C5 setup in front of the glass tank. (B) Top-view schematic of the setup with cameras C1-C5 in front of the glass tank with water. (C) The template attached to the T shaped bar and placed in the glass tank with water as viewed by cameras. (D) Front-view schematic of the glass tank setup with template attached to T-shaped bar moved at different stations $S_1, S_2$ and $S_3$ sequentially. ....	17
<b>Figure 3-4:</b> The Hydro Track 1103 underwater treadmill with its 34 inches wide view window on one side and its capture volume of 55 inches x 21 inches x 51.5 inches ( $l \times b \times h$ ). ....	20
<b>Figure 3-5:</b> Experimental setup and calibration wands. (A) and (B) shows five cameras (C1, C2, C3, C4 and C5) arranged in front of the view window of the aquatic treadmill, (C) Conventional wand provided by Vicon company and (D) Custom wand made for aquatic calibration. ....	22



**Figure 3-6:** Representative schematic for knee and ankle angle definitions associated with the six-marker setup to evaluate lower limb kinematics..... 23

**Figure 3-7:** Knee and ankle angle definitions for clinical interpretations [54]..... 24

**Figure 3-8:** Knee angle during one complete gait cycle and outcomes of interest..... 25

**Figure 3-9:** Ankle angle during one complete gait cycle and outcomes of interest..... 25

**Figure 4-1:** The mean knee and ankle angles for treadmill speeds of 1 (solid lines), 2 (dashed lines) and 3 (dotted lines) mph. (A) and (B) represent the mean knee angles for condition 1 and condition 2, respectively. (C) and (D) represent the mean ankle angles for condition 1 and condition 2, respectively. .... 34

**Figure 4-2:** The variability of the mean knee and ankle angles across a gait cycle in condition 1 (solid black line) and condition 2 (dashed line). (A), (B), and (C) represent the mean knee angles at 1, 2, and 3 mph, respectively, and (D), (E), and (F) represent the mean ankle angles at 1, 2, and 3 mph, respectively..... 37

**Figure 4-5:** Velocity and acceleration of the calf modeled as a circular cylinder during a gait cycle. .... 44

**Figure 4-6:** Estimates of the viscous drag (A), the force due to added mass (B), and total fluid dynamic force (C) over a gait cycle in condition 1 (air) and condition 2 (water)... 45

**Figure 4-7:** Power required to overcome the total fluid dynamic force in a gait cycle. ... 47

## LIST OF TABLES

Table	Page
<b>Table 3-1:</b> Participant Characteristics.....	20
<b>Table 4-1:</b> Medians of each marker distance in the three mediums.....	29
<b>Table 4-2:</b> Accuracy outcomes across the three mediums.....	30
<b>Table 4-3:</b> Kinematic parameters (mean $\pm$ SD) of the gait collected at 1, 2, and 3 mph and the associated results of the statistical analysis to determine the influence of speed for condition 1 and condition 2.....	32
<b>Table 4-4:</b> The mean kinematic parameters of gait collected at 1, 2 and 3 mph and associated results of statistical analyses to determine the influence of the treadmill scenarios of condition 1 versus condition 2.....	36
<b>Table 4-5:</b> The average time for a gait cycle and the corresponding positive mechanical work.....	48
<b>Table B-1:</b> Mean kinematic angles and time measures for knee and ankle joints.....	59



## LIST OF SYMBOLS AND ABBREVIATIONS

SYMBOL	DEFINITION	UNIT
$C_d$	= coefficient of drag	[1]
$d$	= diameter of calf	[m]
$d_1$	= distance between markers $M_r$ and $M_1$	[m]
$d_2$	= distance between markers $M_r$ and $M_2$	[m]
$d_3$	= distance between markers $M_r$ and $M_3$	[m]
$d_m$	= diameter of the marker	[m]
$d_p$	= Euclidean distance	[m]
$F'_{\text{added mass}}$	= force due to added mass (per unit length)	[N/m]
$F'_d$	= viscous drag (per unit length)	[N/m]
$F'_{\text{total}}$	= total fluid dynamic force (per unit length)	[N/m]
DF	= dorsiflexion	[°]
$M'_{11}$	= added mass coefficient (per unit length)	[kg/m]
$M_r$	= reference marker	[]
$M_1$	= marker 1 on template	[]

$M_2$	=	marker 2 on template	[ ]
$M_3$	=	marker 3 on template	[ ]
$P$	=	Precision	[m]
$Re$	=	Reynolds Number	[1]
ROM	=	range of motion	[°]
$S_q$	=	station number	[ ]
$T$	=	Trueness	[m]
$v$	=	velocity of tibia marker	[m/s]
$W^+$	=	positive mechanical work	[J/m]
$\rho$	=	density of fluid	[kg/m <sup>3</sup> ]
$\mu$	=	dynamic viscosity of fluid	[N s/m <sup>2</sup> ]

## **CHAPTER 1**

### **INTRODUCTION**

#### **1.1 Background and Motivation**

Recent studies in clinical rehabilitation have demonstrated the potential benefits of aquatic-based therapies, including exercise in an underwater treadmill [1–3], in comparison to land-based therapies [1,4,5]. Factors like density, specific gravity, buoyancy, and other physical principles of water contribute to the advantages of performing physical exercises in an aquatic environment [5]. Rehabilitation scenarios have progressed towards trying to evaluate the patterns of locomotion while underwater [6,7]. However, in order to quantify these effects, it is important to understand human locomotion in an aquatic environment.

Motion capture (mo-cap) is one of the most common methodologies used in biomechanical analysis [8,9]. While this instrumentation plays a vital role in areas such as clinical gait analysis to improve treatment of injuries and medical conditions such as lower limb amputation, it can also be used to address other clinical problems, such as treatment of neuromuscular disorders and cerebral palsy [10]. Mo-cap systems use different



methodologies to collect and analyze human locomotion [11]. The reliability and validity of data from such mo-cap systems has continued to be an area of interest among the scientific community [12–15]. In the past decade the assessments of mo-cap systems for validity have been predominantly performed on systems that utilize the tracking of retro-reflective marker positions in three-dimensional (3-D) space [14,15].

The aforementioned studies have been limited to land-based applications. Conducting mo-cap underwater can be a challenge because the default retro-reflective markers provided by the system manufacturers lose their retro-reflective properties immediately after they are submerged and wetted. This necessitates identifying a potential material that could retain its retro-reflectivity when submerged in water for aquatic applications.

## **1.2 Research Objectives**

The overall objective of this study is to realize a methodology to quantify lower limb kinematics during an aquatic treadmill session using a land-based mo-cap system. As emphasized in the literature review (Chapter 2), there is a need to understand the effect of aquatic environment on the lower limb motion, known as gait. Consequently, kinematics of lower limb motion were studied while walking on a treadmill in the presence of water in comparison to kinematic outcomes while walking on a treadmill without water.

The specific objectives of the research are as follows:

- To choose a retro-reflective marker material capable of preserving the retro-reflective capabilities when submerged. We evaluate the implications of static



accuracy of a Vicon T40s mo-cap system in reconstruction of marker distances in an aquatic environment weighed against similar measurements without water.

- To assess the walking kinematics from a biomechanics stand-point, by processing the motion data to obtain gait angles (knee and ankle) in the sagittal plane. We make observations of differences in gait patterns over land and in water and analyze its implications.
- To quantify resistive effects by estimating total fluid dynamic force in water. We model the total fluid dynamic force by estimating the viscous drag and the added mass assuming the calf of the leg to be a 2-D cylinder.

The approach used to meet the objectives of this thesis is as follows. Accuracy outcomes were studied by arranging the mo-cap cameras in front of a glass tank. A measurement template was created using retro-reflective markers and placed in the tank. Marker center distances were recorded both with and without the presence of water in the glass tank. For kinematic assessments, thirteen participants were recruited based on Institutional Review Board (IRB) protocols for utilization of human subjects in this study. The participants were requested to walk at 1, 2 and 3 mph and their motion data were captured both in a treadmill session without water and with water. Furthermore, effects of the presence of water on the motion were analyzed and interpreted using statistical analysis using parametric testing procedures: Repeated Measures Analysis of Variance (RMANOVA) and Paired t-tests. Friedman ANOVA was used as the non-parametric testing procedure. The total fluid dynamic forces were estimated in terms of viscous drag and added mass to interpret the greater time required to complete a gait cycle in water in comparison to in air.

### **1.3 Thesis Outline**

The organization of this thesis is as follows. In Chapter 2, an extended literature review is presented addressing the importance and relevance of this study. In Chapter 3, the materials and methodology used to conduct this investigation are introduced by describing the arrangement of cameras, calibration and mo-cap data processing, the method of analysis with appropriate equations used, and the experimental methodology used for kinematic assessments on the treadmill. Results and discussions are shown in Chapter 4, where the analysis of gait patterns are reported along with the outcomes of the accuracy analysis. Chapter 5 provides the conclusions and future work based on the results and discussions.

### **1.4 Content Disclaimer**

Part of the contents and figures pertaining to accuracy analysis in this thesis are taken from the following reference, co-authored by the author of this thesis.

- Raghu, S. L., Kang, C., Whitehead, P., Takeyama, A., and Conners, R., “Static accuracy analysis of Vicon T40s motion capture cameras arranged externally for motion capture in constrained aquatic environments,” *Journal of Biomechanics*, vol. 89, May 2019, pp. 139–142.

The author of this thesis has the right to reproduce the figures and text from the above publication with appropriate citations.



## **1.5 Human Subjects Research**

This study was approved by the IRB of The University of Alabama in Huntsville. The subjects were informed about all the procedures and potential risks prior to participation in this study after which a written informed consent was obtained according to IRB protocols. The IRB approval is attached in Appendix A.

## **CHAPTER 2**

### **LITERATURE REVIEW**

#### **2.1 Motion Capture and Human Locomotion**

Motion capture has been proven to be useful in many applications such as entertainment [16], biomechanics [17] and sports [18]. Mo-cap has played a vital role in evaluation of human locomotion. Marey [19] and Muybridge [20] were pioneers who quantified human locomotion by analyzing series of photographs taken at different instances of locomotion. Over time, the advent of new instruments and technologies has enabled development of different mo-cap methodologies.

Traditionally, mo-cap can be divided into two categories: Optical mo-cap (OMC) and Inertial mo-cap (IMC) (see Figure 2-1). Typically, OMC is used in a laboratory context while an IMC is used in an ambulatory context [21].



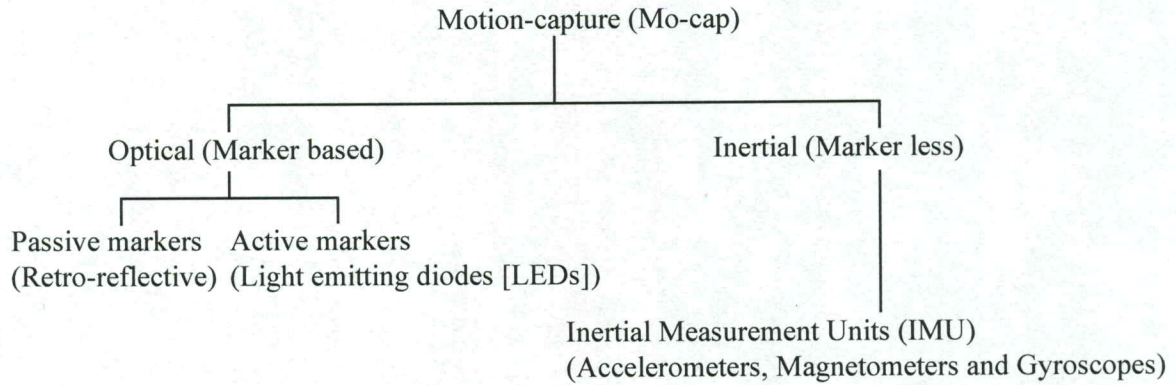


**Figure 2-1:** Classification of important motion capture methods.

OMC technology typically uses infrared (IR) cameras and markers to perceive human movement in 3-D [22]. This approach uses either active markers (LEDs) or passive markers (retro-reflective markers). Markers are strategically placed at anatomical regions of interest.

IMC technology use Inertial Measurement Units (IMU) to perceive human movement [23] that generally comprises of accelerometers, magnetometers and gyroscopes to record kinematic data. The key challenge in IMC is to obtain the position of the subject with respect to a fixed frame [21]. In addition, IMC is not widely used in clinical gait analysis because the technologies are not well developed and their accuracy is doubtful [24]. On the other hand, OMC systems are known to have sub-millimeter accuracy making them the preferred systems to evaluate human locomotion [14,25]. This study utilizes a Vicon OMC system composed of T40s cameras (Vicon Motion Systems, LA, USA) and software which record the motion of the passive markers (retro-reflective) placed on the anatomical regions of interest such as the bony landmarks for lower limb (mid-thigh, lateral joint line – knee, mid-fibula – calf, calcaneus – heel, lateral malleolus – ankle, and second metatarsal – toe) and produce a 3-D trajectory.

## 2.2 Analysis of Human Locomotion

Biomechanics of human movement forms the fundamental baseline for the analysis of human locomotion [26]. The biomechanics of human movement can be analyzed from two perspectives: kinematics or kinetics [21]. The kinematics describe the movement of body segments neglecting the masses. The kinematic quantities can be a combination of both linear components (position, linear velocity, and linear acceleration) and angular components (orientation, angular velocity, and angular acceleration). On the other hand, kinetics deals with the measurement of linear forces and angular moments.

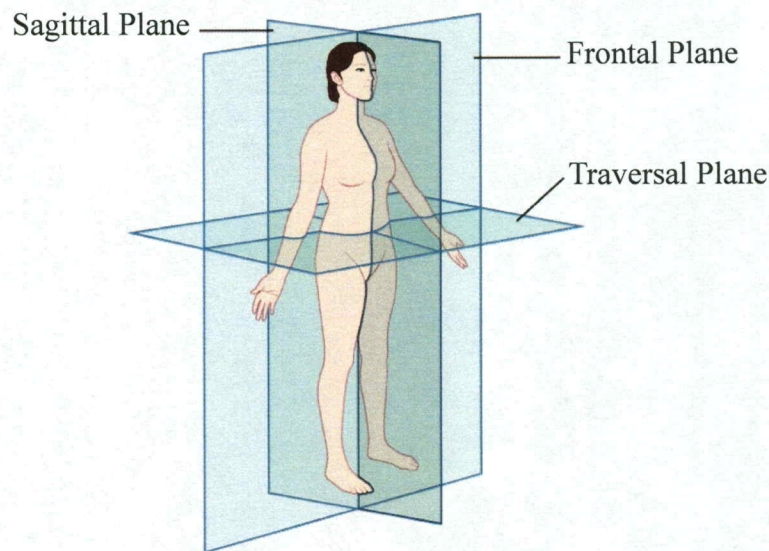


**Figure 2-2:** Anatomical planes of the body [27].

The systematic evaluation of human locomotion is also referred to as gait analysis [28]. Gait is defined as an individual's manner of walking and is described in terms of three planes: sagittal, frontal, and transverse plane [29] (see Figure 2-2). Gait analysis forms one of the basic assessment techniques to determine functional independence of a human subject [30]. The main purpose of 3-D motion capture is to determine, and preferably



quantify, this functional independence of a human subject. Gait analysis also plays a vital role in addressing various clinical problems such as treatment of injuries and conditions of the musculoskeletal system, treatment of neuromuscular disorders and cerebral palsy [10]. The gait information in the sagittal plane has been the focus of most human movement studies [31–34]. Figure 2-3 illustrates the events during a complete gait cycle. A gait cycle is characterized by two phases; the stance phase and the swing phase. Stance phase refers to the interval of time feet remain on ground which normally corresponds to 60% of the gait cycle. The remainder of 40% (toe-off to successive heel strike) corresponds to the swing phase of the gait cycle [35]. In this study, gait analysis in the sagittal plane also forms the basis of all the reported kinematic results and discussion.

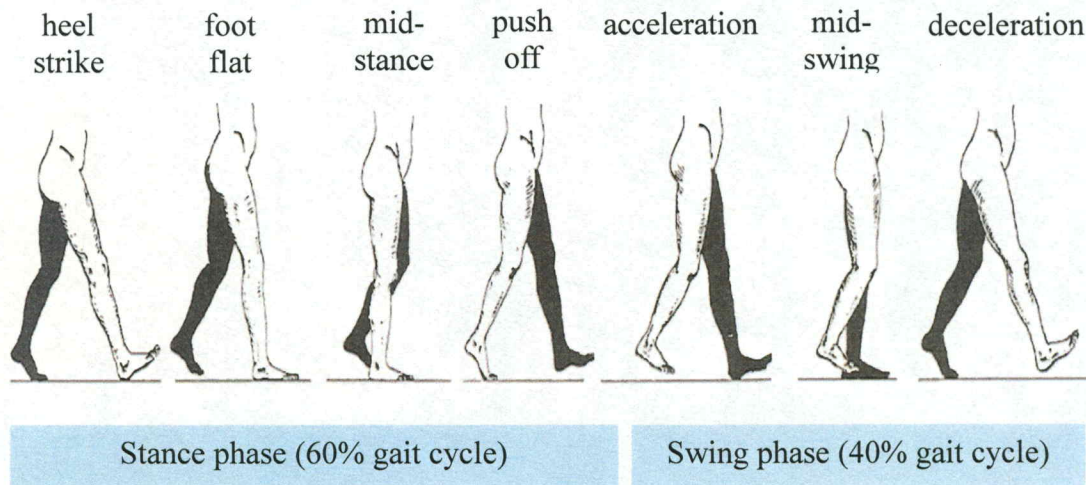


**Figure 2-3:** Illustration of a complete gait cycle and gait events.

### 2.3 Human Locomotion in Water and Aquatic Rehabilitation

Recently, locomotion in water has become the preferred medium for exercise routines by clinicians and trainers in clinical rehabilitation programs [5,36–38]. Fluid



mechanical properties such as buoyancy and drag play a decisive role in this choice. The buoyancy force counteracts the force due to gravity while the drag is the resistive force opposing the movement of the limb through the water. While, buoyancy helps in offloading the full load of the body, the resistive force (drag) helps in enhanced control of the movement of the limb [5,36]. These unique characteristics form the fundamental baseline and motivation of aquatic therapy or clinical rehabilitation using a water medium.

The drag and buoyancy forces are affected by density, specific gravity, hydrostatic pressure, and thermodynamics [5]. Water is nearly 800 times denser than air, therefore, the drag magnitude in water is 800 times more than in air. On the other hand, the thermodynamic properties of water make it a unique exercise medium compared to air. While water has the ability to retain heat, it can also more effectively transfer heat energy. For this reason, water constitutes a natural therapeutic medium for rehabilitation [5].

The water environment for rehabilitation can be provided by two means: walking in a swimming pool or in a self-contained unit such as an underwater treadmill. It is difficult to fix physical and physiological intensity while walking/running in a swimming pool [39]. On the other hand, in a self-contained unit such as, a treadmill in a tank of water, the speed of the walking can be controlled. Additionally, use of an aquatic treadmill enables functional improvements such as additional water jets to add more resistance during a rehabilitation program [38]. Therefore, an aquatic treadmill is an effective exercise unit as it offers better control over locomotion that can also be customized according to requirement of a participant undergoing rehabilitation.



The emergence of aquatic based approaches for rehabilitation establishes the need for researchers to quantify its effects and maximize the benefits of a structured rehabilitation program. This necessitates analysis and understanding of locomotion in water from two important perspectives: the medical standpoint (psychological, metabolic, cardiorespiratory, neurological, muscular etc.,) and the biomechanical standpoint (kinematics and kinetics) [10,37].

From a medical standpoint, psychological [40], cardiorespiratory [41,42], metabolic [2,3], muscular [37] and neurological [2] effects of a water environment for clinical rehabilitation have been previously reported. This has helped researchers in establishing clinical relevance of aquatic therapy for rehabilitation programs. Aquatic therapy not only helps older adults with medical conditions, it has also gained popularity among younger groups of people and athletes for recovery from lower limb injuries and strength training [32].

Clinical relevance of aquatic rehabilitation has motivated researchers towards trying to understand the locomotion of legs in an aquatic environment from a biomechanical standpoint. Although the clinical relevance of biomechanical parameters of human locomotion in water has not yet been established, there is a growing body of literature in this area of research [26,36–38].

The biomechanical standpoint involves both the aspects of kinematics and kinetics as discussed in section 2.2. As discussed in section 2.1, mo-cap has been often used in biomechanics but for in air applications (over the land) [31,34,43,44]. However, evaluating

biomechanics in water is challenging as most instruments are not built to operate in an aquatic environment [36].

Efforts have been made to develop a systematic framework for 3-D motion analysis underwater [6,7]. However, the reliability of such systems has not been demonstrated for clinical applications such as gait analysis. There are state-of-the-art mo-cap systems that are specifically suited for underwater water purposes such as Oqus cameras (Qualisys, Goteberg, Sweden) [32]. However, such systems may not be well suited for all the aquatic applications as the cameras are too large to be housed in smaller capture volumes. In addition, use of underwater cameras in smaller capture volumes restricts the viewing angles for accurate mo-cap. For example, it would be easier to use an extensive underwater system if the trials are based in a swimming pool with a large volume. On the other hand, self-contained units like an aquatic treadmill have a smaller volume restricting the use of underwater motion capture systems.

There are only two studies [32,45] that have measured the kinematic aspects of gait in water in comparison to air. Jabbar *et al.* [32] used Oqus cameras in a large swimming pool, whereas Barela *et al.* [45] used digital cameras and digitization techniques to decipher locomotion in water. The possibility of using OMC systems to reconstruct markers submerged inside an aquatic environment has not been explored. Additionally, the evaluation of the accuracy of mo-cap systems is a developing area of research [14,15,46] that often depends on a laboratory context and is application specific. Hence, usage of land-based mo-cap systems for aquatic applications also necessitates the requirement to evaluate the accuracy in reconstruction of markers in a submerged environment.



This study taps this underexplored area of research by using a Vicon OMC (Vicon Motion Systems, LA, USA) with T40s cameras to reconstruct markers in an aquatic environment (underwater treadmill). The accuracy of the OMC system is systematically evaluated for the lower limb gait analysis.

## CHAPTER 3

### MATERIALS AND METHODS

#### 3.1 Accuracy Analysis

##### 3.1.1 *Cameras, Markers, and Template*

The tests were performed using five stand-mounted Vicon T40s cameras. The potential material that could retain its retro-reflectivity when submerged in water was found to be 3M™ Scotchlite™ Reflective tape, Safety of Life at Sea (SOLAS) Grade 3150 – A. This commercially available tape was cut in the form of equally sized petals and wound around each spherical marker of 14 mm diameter ( $d_m$ ; [Figure 3-1A]). A small patch of SOLAS tape was adhered to conceal the uncovered portions of the top surface of the marker. A template was created by attaching five custom-made markers in a mirrored L-shape. Four markers ( $M_r$ ,  $M_1$ ,  $M_2$ , and  $M_3$ ) were used for the evaluation of static distances (Figure 3-1B). The fifth marker was not used to avoid repetition of similar distances. The static accuracy analysis was based on three static distances ( $d_1$ ,  $d_2$ , and  $d_3$ ) between the marker centers as perceived by the Vicon T40s cameras (Figure 3-1B). The distances



between these markers were measured with Vernier calipers to provide the reference values in the static accuracy analysis:  $(d_1)_{ref} = 27$  mm,  $(d_2)_{ref} = 52$  mm and  $(d_3)_{ref} = 73$  mm.

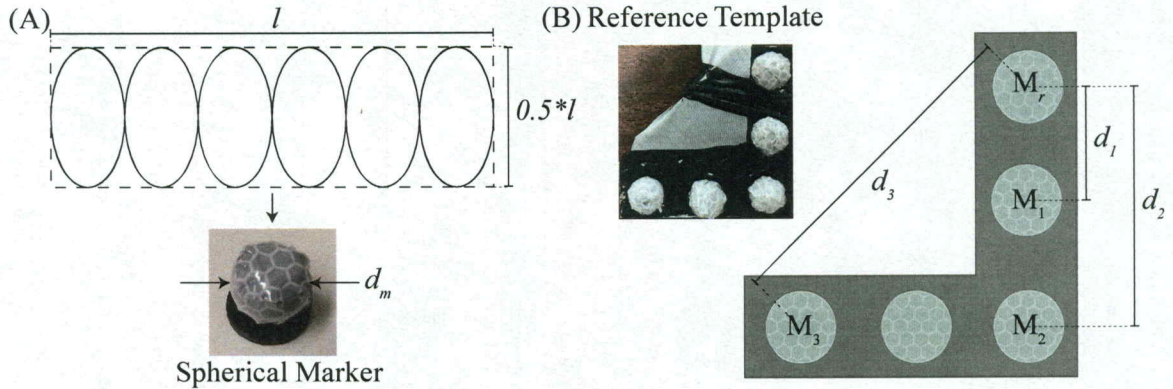


**Figure 3-1:** Marker creation and reference template for static measurements. (A) SOLAS reflective tape cut into petals of equal sizes wound around a spherical marker (length,  $l = \pi d_m = 43.98$  mm). (B) Static reference template used for analysis with measured distances between marker centers; ( $d_1$ : Distance between markers  $M_r$  and  $M_1$ ;  $d_2$ : Distance between markers  $M_r$  and  $M_2$ ;  $d_3$ : Distance between markers  $M_r$  and  $M_3$ ).

### 3.1.2 Calibration, Setup, and Processing

The system calibration was performed using a Vicon wand (Figure 3-2) with all five cameras arranged in a curved row (Figure 3-3A & 3-3B). The Vicon wand is a T-shaped tool with five precisely spaced retro-reflective markers provided for routine calibration. The calibration was performed by waving the wand in the field of view of the cameras in air medium. This was since the available capture volume (glass tank) for calibration is small, which restricts the movement of the calibration wand in the capture volume.

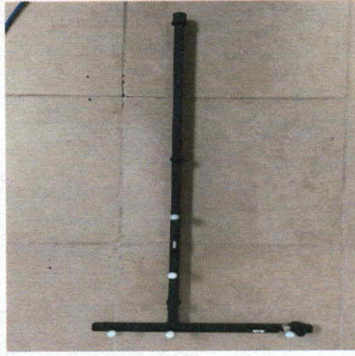


**Figure 3-2:** Vicon wand with five precisely spaced markers.

Following camera calibration, an origin was set using the same wand on a table aside the glass tank for further assessments (Figure 3-3B and 3-3C). This origin acts as a reference frame for position data. A glass tank with dimensions of  $610 \times 300 \times 410 \text{ mm}^3$  and glass thickness of 4.90 mm was placed on a table facing the cameras. The static reference template was attached to metallic bars in the shape of a T and mounted on top of the tank (Figure 3-3C). The Nexus software was used for calibration and collect marker position data. Analysis of the position data was performed with MATLAB (Version R2016b).



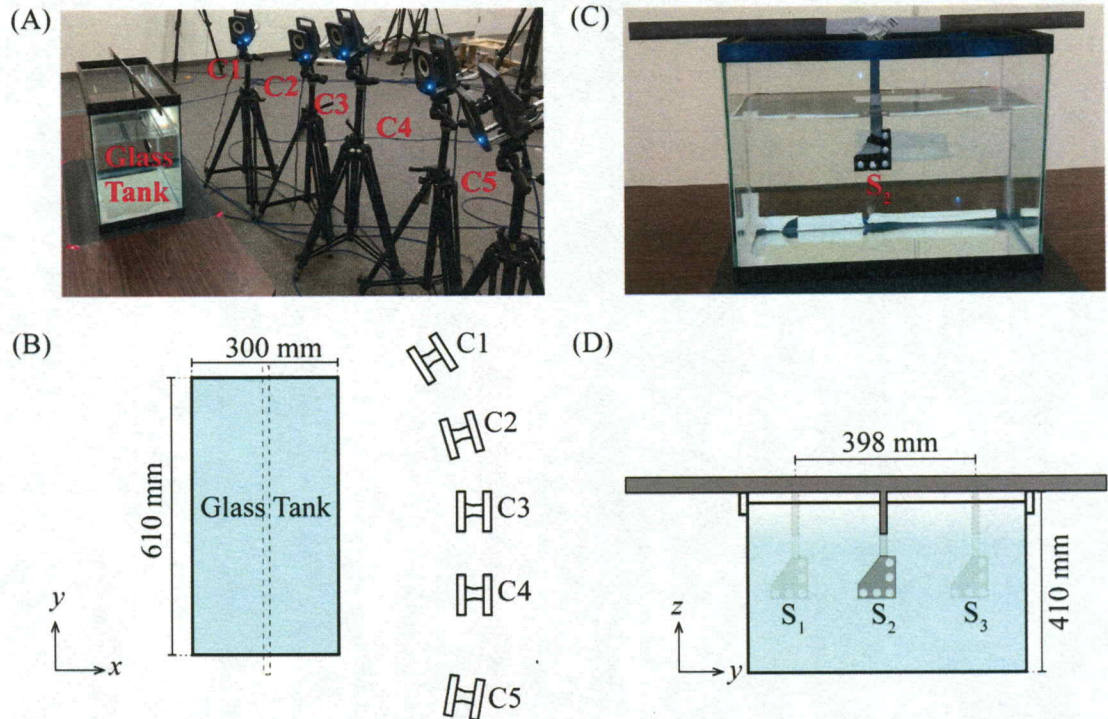


**Figure 3-3:** Experimental setup and test schematic. (A) Cameras C1-C5 setup in front of the glass tank. (B) Top-view schematic of the setup with cameras C1-C5 in front of the glass tank with water. (C) The template attached to the T shaped bar and placed in the glass tank with water as viewed by cameras. (D) Front-view schematic of the glass tank setup with template attached to T-shaped bar moved at different stations  $S_1, S_2$  and  $S_3$  sequentially.

### 3.1.3 Procedure

The aim of the first series of test was to evaluate the static distances between the marker centers on the template in three scenarios: in air (*air*), in the glass tank without water (*glass*), and in the glass tank filled with water (*water*). Three stations  $S_1, S_2$  and  $S_3$  were marked at different lateral locations across the glass tank (Figure 3-3D). The static reference template was sequentially placed at these stations and the data was recorded at a sampling rate of 200 Hz [14]. The data was first recorded by placing the reference template



in air outside the glass tank (*air*) at all three stations. The template was next placed inside the tank without water (*glass*) and moved to all three stations. Finally, the tank was filled with water, and the template was again placed at all three stations (*water*). At each station, the position data ( $x$ ,  $y$  and  $z$ ) was recorded during three trials lasting one second per trial. The recorded data was then processed using pipeline operations in Nexus to yield the position data with respect to the set origin as a comma separated value (CSV) file.

#### 3.1.4 Method of Analysis

The coordinates of the marker centers in the CSV file were processed using a MATLAB script to calculate the Euclidean distances. The Euclidean distances  $d_p$  at each station  $S_q$  between the marker centers were calculated by Eq. 3-1

$$d_p = \sqrt{(\bar{x}_{M_i} - \bar{x}_{M_j})^2 + (\bar{y}_{M_i} - \bar{y}_{M_j})^2 + (\bar{z}_{M_i} - \bar{z}_{M_j})^2}. \quad (3-1)$$

Here,  $p$  and  $q$  represent the marker distance index and station index respectively. Also, subscript  $i$  represents the marker index with  $i = 1, 2,$  and  $3$ ;  $\bar{x}$ ,  $\bar{y}$  and  $\bar{z}$  represent the average value of coordinates of the marker centers obtained through Vicon in one second (200 frames).

The Trueness  $T$  for each scenario were calculated using Eq. 3-2 as mean marker distance error of the three distances measured at all three stations with respect to the reference values.

$$T = \frac{1}{m} \sum_{p=1}^m \left[ \frac{1}{N} \sum_{q=1}^N \left| (\bar{d}_p)_{S_q} - (d_p)_{ref} \right| \right]. \quad (3-2)$$

Here,  $m = 3$  and  $N = 3$  represent the number of marker center distances and number of stations respectively and  $\bar{d}_p$  represents the mean distance obtained between the appropriate marker centers in three trials.

Precision  $P$  were calculated using Eq. 3-3 as mean standard deviation of mean marker distances measured by Vicon cameras.

$$P = \left( \frac{1}{m} \right) \sum_{p=1}^m \left[ \sqrt{\frac{1}{N-1} \sum_{q=1}^N \left( \mu_p - (\bar{d}_p)_{S_q} \right)^2} \right], \quad (3-3)$$

where  $\mu_p$ , the average marker distance at each station were calculated by Eq. 3-4.

$$\mu_p = \frac{1}{N} \sum_{q=1}^N (\bar{d}_p)_{S_q} \quad (3-4)$$

Trueness  $T$  in Eq. 3-2 and Precision  $P$  in Eq. 3-3 for each medium is obtained on similar lines to Trueness and Precision in Eichelberger *et al.* (2016) respectively [14].

Due to the size of the sample, marker distance and accuracy outcomes across mediums were analyzed using Friedman analysis of variance (ANOVA), a non-parametric repeated measures testing procedure [47]. This was done in order to assess the influence of mediums in measurement of distances and accuracy outcomes. The analyses were performed using the IBM Statistical Package for the Social Sciences (SPSS) Statistics, Version 25. Level of significance was set at  $p < 0.05$ .



## 3.2 Kinematic Analysis

### 3.2.1 Participants

Thirteen college-aged able-bodied individuals (6 males and 7 females) were recruited based on random sampling. The physical characteristics of participants recruited in this study are listed in Table 3-1.

**Table 3-1:** Participant Characteristics.

	Age (years)	Height (m)	Weight (kg)
Male ( $n = 5$ )	$25.4 \pm 3.9$	$1.8 \pm 0.05$	$76.1 \pm 6.8$
Female ( $n = 7$ )	$21.3 \pm 2.3$	$1.7 \pm 0.05$	$69.7 \pm 13.5$
All participants ( $n = 12$ )	$23.0 \pm 3.6$	$1.7 \pm 0.08$	$72.3 \pm 11.3$

Each individual walked at speeds of 1 mph, 2 mph, and 3 mph on a Hydro Track 1103 underwater treadmill (HydroTrack<sup>®</sup>, Conray Inc., Phoenix, AZ, USA). Figure 3-4 shows the treadmill and a schematic of the tank volume.

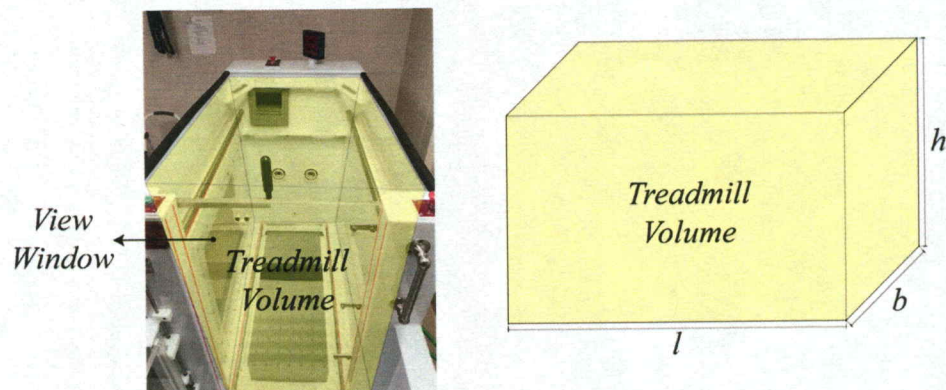


**Figure 3-4:** The Hydro Track 1103 underwater treadmill with its 34 inches wide view window on one side and its capture volume of 55 inches x 21 inches x 51.5 inches ( $l \times b \times h$ ).



Participants performed walking in two different conditions: condition 1 - treadmill runs without water; and condition 2 - treadmill runs with the tank filled with water. For condition 2, the water level was consistently adjusted to be waist-high for all the participants. The water temperature for all the trials in condition 2 was maintained at 90 °F. Motion capture data could not be used for one male participant due to operational difficulties during the aquatic treadmill session.

### 3.2.2 *Cameras, Calibration, Setup and Processing*

The experimental setup consisted of five Vicon T40s cameras (Figures 3-5A and B). As discussed in section 3.1.2, the camera calibration was performed in air for condition 1. Because the conventional wand (Figure 3-5C) is not suited for water, calibration for condition 2 was performed using a custom wand made by using SOLAS markers (Figure 3-5D). The dimensions of this wand were consistent with the conventional wand.



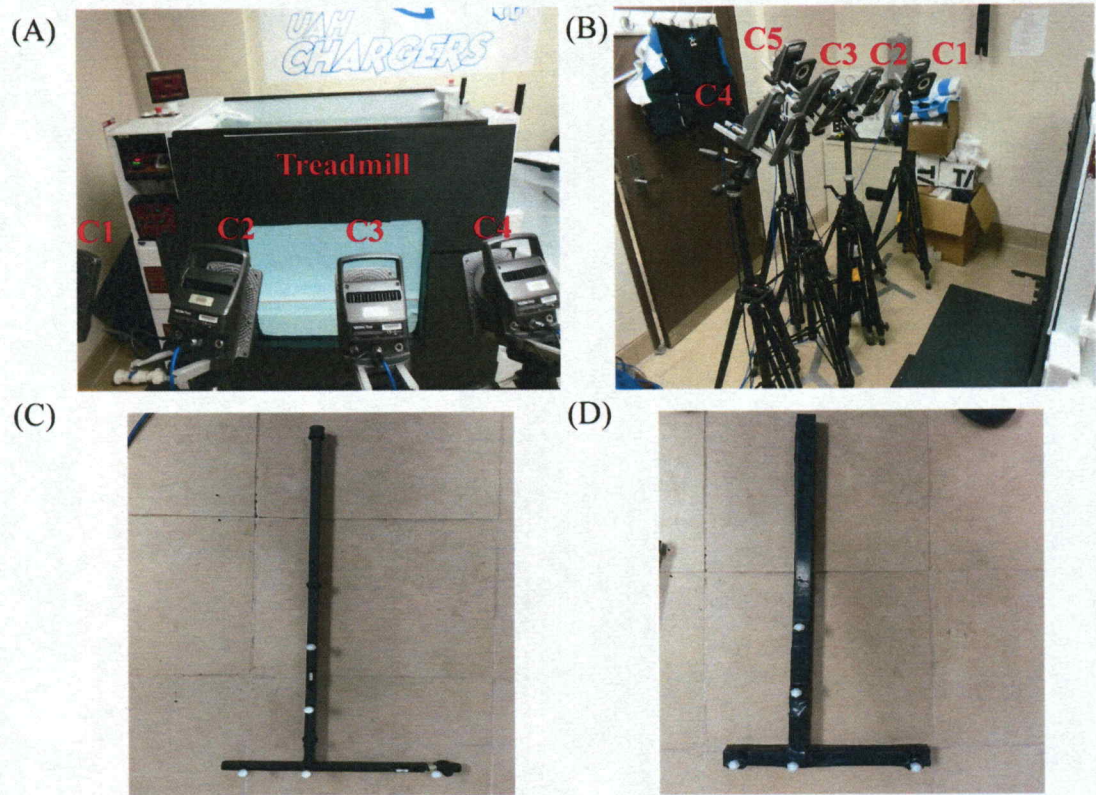


**Figure 3-5:** Experimental setup and calibration wands. (A) and (B) shows five cameras (C1, C2, C3, C4 and C5) arranged in front of the view window of the aquatic treadmill, (C) Conventional wand provided by Vicon company and (D) Custom wand made for aquatic calibration.

Six markers were setup on bony landmarks on the lower limb to represent the knee and ankle angle joints (see Figure 3-6). Five trials were recorded at each speed at a sampling frequency of 100 Hz [1,43,48] unlike accuracy analysis where trials were recorded at a sampling frequency of 200 Hz. Trials conducted on all the participants were processed using Nexus software to yield the position data. For condition 1 (treadmill runs without water), a woltring quintic spline interpolation [49] was used for no more than five frames of missing marker data. For condition 2, woltring spline interpolation was used for no more than ten frames of missing marker data. All marker position data were smoothed



using a 4<sup>th</sup> order Butterworth low-pass filter with cut-off frequency of 6 Hz that is conventionally used for gait analysis in biomechanics [31,50,51].

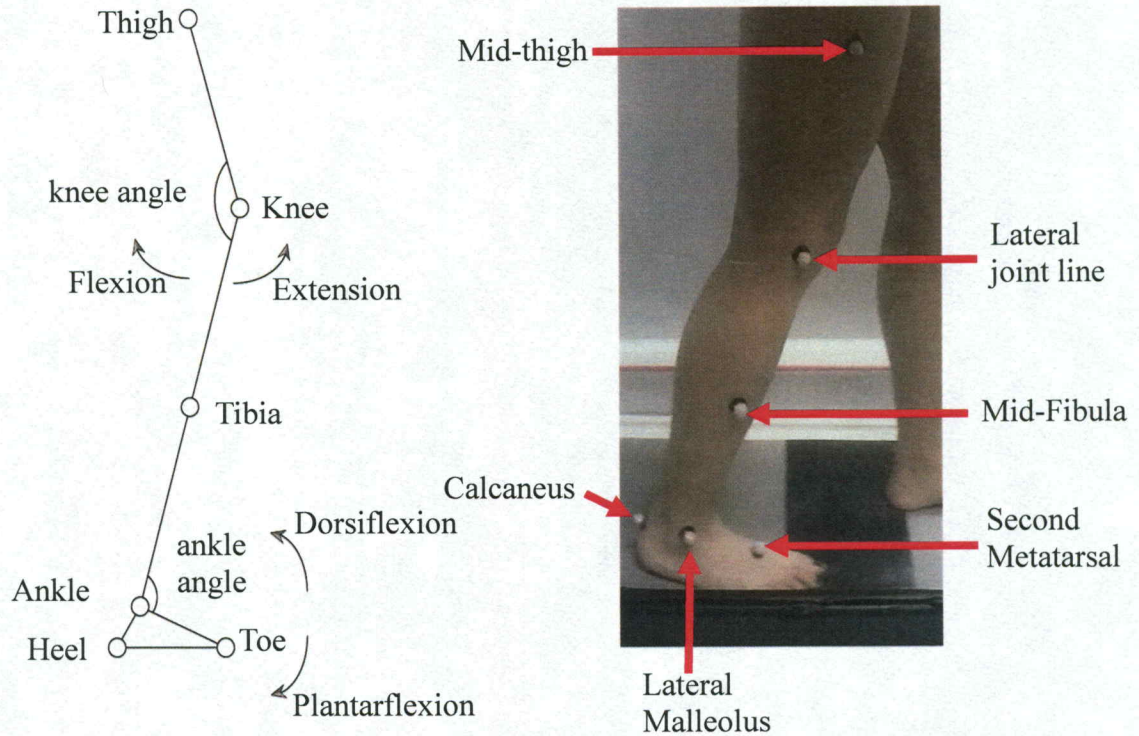


**Figure 3-6:** Representative schematic for knee and ankle angle definitions associated with the six-marker setup to evaluate lower limb kinematics.

### 3.2.3 Kinematic and Statistical Analysis

The knee and ankle angles (Figure 3-6) were estimated from the Vicon position data using a custom built MATLAB script. Three consecutive gait cycles were selected from the gait time history and time normalised to 101 points per gait cycle [52]. The normalized gait cycles were further averaged for five trials at each speed of 1, 2 and 3 mph respectively. The gait events for normalisation (start and end of the gait cycle) are detected



based on a velocity based treadmill algorithm [53]. The gait cycle begins at the start of a heel strike and ends with a successive heel strike.

Figure 3-7 illustrates knee and ankle angle definitions. For clinical interpretation, the knee angle is measured in terms of flexion and extension and the ankle angle is measured in terms of dorsiflexion (DF) and plantarflexion (PF).

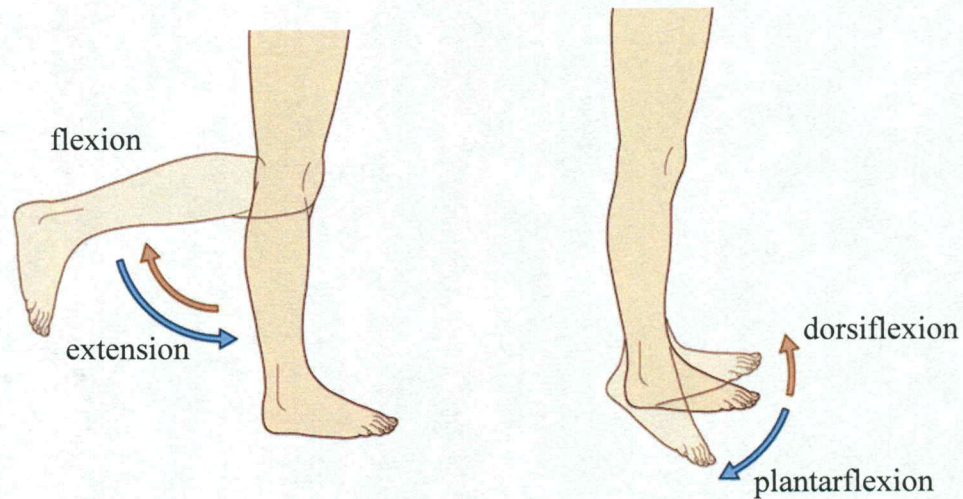


**Figure 3-7:** Knee and ankle angle definitions for clinical interpretations [54].

The overall kinematic analyses were based on processed gait information of the dominant leg of the participant. The dominant leg was assessed using a survey by posing a question on the foot an individual would prefer to use to kick a football [55]. Most of the participants preferred to use the right foot except for one female participant who preferred the left foot. Figures 3-8 and 3-9 illustrate the typical behavior of knee and ankle angles in a gait cycle and the outcomes of interest in this study. The relative motion of the leg is illustrated in each Figure to highlight the nature of the leg motion during different intervals of gait cycle. The gait information for the dominant leg was processed for the knee: peak

flexion, time to peak flexion and range of motion (ROM); and for the ankle: peak dorsiflexion (DF), time to peak DF and ROM.

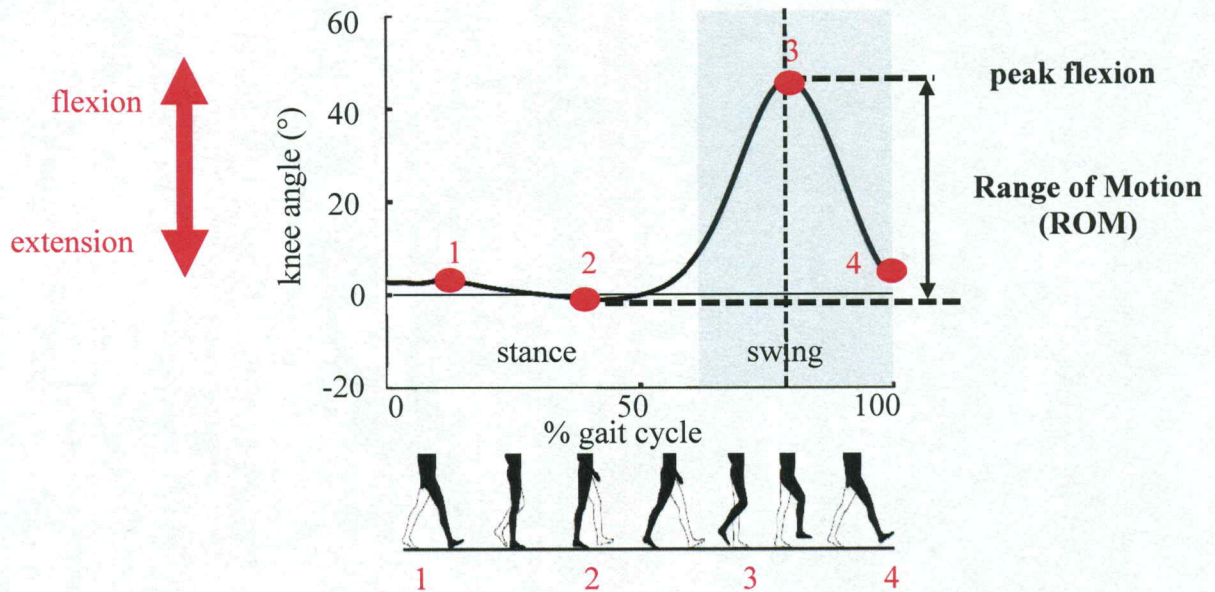


**Figure 3-8:** Knee angle during one complete gait cycle and outcomes of interest.

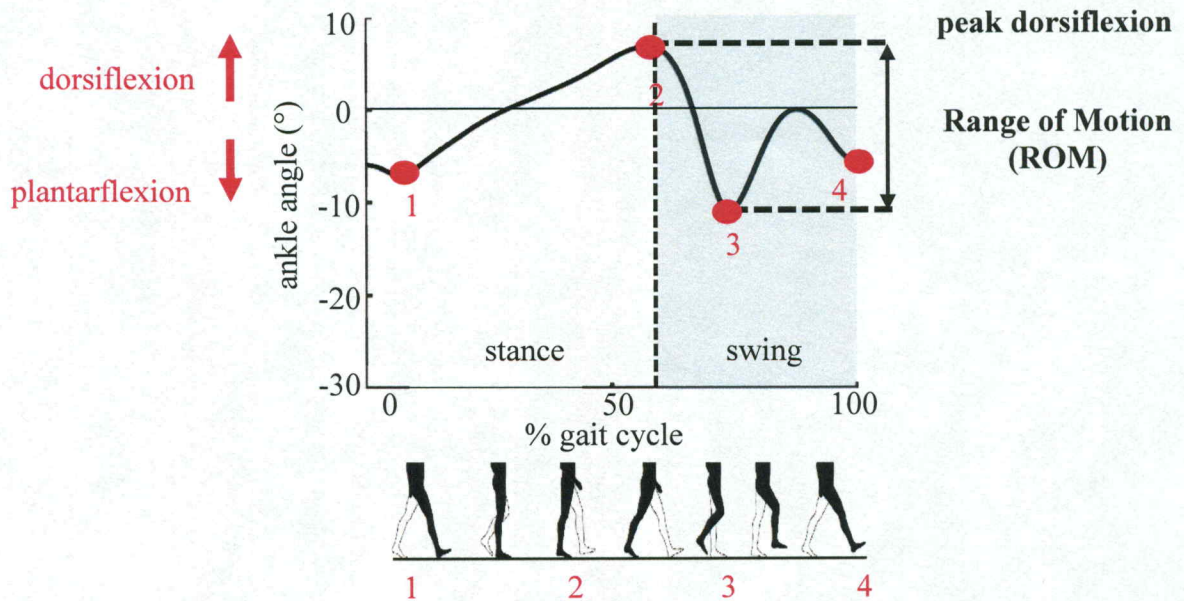


**Figure 3-9:** Ankle angle during one complete gait cycle and outcomes of interest.



Normality of the gait measures was tested using the Shapiro-Wilk tests [56]. The normality of data was established by the level of significance  $p$ . If  $p < 0.05$ , the data is normally distributed. If  $p > 0.05$ , the data is not normally distributed.

Repeated measures analysis of variance (RMANOVA) [57] were conducted on peak flexion, time to peak flexion and ROM for the knee and on peak DF, time to peak DF and ROM for the ankle at treadmill speeds of 1, 2 and 3 mph, respectively. This allowed us to identify significant differences for normally distributed data [56]. Typically, the statistical results of RMANOVA is represented in terms of the  $F$  statistic value, degrees of freedom  $df$  and the level of significance  $p$ . The  $F$  statistic value helps to determine the validity of the null hypothesis (there is no effect of treadmill speed on the knee and ankle kinematic outcomes). If the null hypothesis is true,  $F$  is likely to be closer to 1.0. If the null hypothesis is false, then the value of  $F$  is likely to be greater than 1.0. The number of degrees of freedom ( $df$ ) is the number of independent ways that the dynamic nature of outcomes can move, without violating the constraint imposed on it. The level of significance  $p < 0.05$  indicates statistically significant differences in the outcomes while  $p > 0.05$  indicates no statistically significant difference. If data were not normally distributed, a Friedman ANOVA [57] was utilized. Pairwise comparisons were utilized to further analyze significant differences across the three speeds.

To analyze the significant influences of the exercise medium at all three treadmill speeds, paired sample  $t$ -tests [58] were used with the three dependent measures for the knee (peak flexion, time to peak flexion and ROM) and the ankle joint (peak DF, time to peak DF and ROM) for both condition 1 (treadmill runs without water - *air*) and condition 2 (treadmill runs with water - *water*).

The statistical results of paired sample *t*-tests are represented in the same way as RMAOVA except for *T* statistic value in lieu of *F* statistic value. The *T* statistic value compares the means of two populations while the *F* statistic value compares the variances of two different populations (*air* vs. *water*).



## CHAPTER 4

### RESULTS AND DISCUSSION

#### 4.1 Accuracy Analysis

##### 4.1.1 Calibration: Marker Distance Outcomes

The mo-cap system calibration procedure was described in section 3.1.2. A glass tank was used along with an L-shaped template with attached retro-reflective markers mounted at known relative distances. Table 4-1 shows the median marker distances and associated interquartile ranges perceived by Vicon T40 cameras with the template placed in the three mediums of *air* (outside the glass tank), *glass* (inside the glass tank without water), and *water* (inside the glass tank with water) with respect to the reference distances  $(d_1)_{ref} = 27.00$  mm,  $(d_2)_{ref} = 52.00$  mm, and  $(d_3)_{ref} = 73.00$  mm (section 3.1.1). The difference in the marker distances for all three mediums is less than 1 mm. Furthermore, Friedman ANOVA revealed no significant difference in three mediums with marker distances:  $d_1$  ( $p = 0.368$ ),  $d_2$  ( $p = 0.264$ ), and  $d_3$  ( $p = 0.264$ ) (see Table 4-1).

**Table 4-1:** Medians of each marker distance in the three mediums.

Distance	Medium	Median	Interquartile range (IQR)		<i>p</i> - value
			25 <sup>th</sup> percentile	75 <sup>th</sup> percentile	
<i>d</i> <sub>1</sub> (mm)	<i>air</i>	26.790	26.783	26.836	0.368
	<i>glass</i>	26.751	26.745	26.752	
	<i>water</i>	27.120	26.683	27.179	
<i>d</i> <sub>2</sub> (mm)	<i>air</i>	51.722	51.689	51.727	0.264
	<i>glass</i>	51.685	51.618	51.757	
	<i>water</i>	51.758	51.678	52.460	
<i>d</i> <sub>3</sub> (mm)	<i>air</i>	72.645	72.608	72.775	0.264
	<i>glass</i>	72.778	72.670	72.930	
	<i>water</i>	72.751	72.595	73.317	

#### 4.1.2 Accuracy Outcomes

The accuracy outcomes for the three marker distances in the three mediums are listed in Table 4-2. The overall trueness (*T*) and precision (*P*) are calculated as the mean trueness and precision of the three marker distances listed in Table 4-2 for each medium. The mean values of *T* for *air* ( $0.270 \pm 0.074$  mm), *glass* ( $0.257 \pm 0.087$  mm), and *water* ( $0.290 \pm 0.106$  mm) are based on Eq. 3-2, and the means of *P* for *air* ( $0.046 \pm 0.036$  mm), *glass* ( $0.068 \pm 0.063$  mm), and *water* ( $0.360 \pm 0.081$  mm) are based on Eq. 3-3 and Eq. 3-4. The Friedman ANOVA on trueness outcomes revealed no significant difference for *d*<sub>1</sub> ( $p = 0.264$ ), *d*<sub>2</sub> ( $p = 0.717$ ), and *d*<sub>3</sub> ( $p = 0.264$ ) in each medium. Therefore, the resultant mean precision calculated as the mean standard deviation of the mean marker distances at



different locations varied between 0.046 mm and 0.360 mm in the three mediums (Table 4-2).

**Table 4-2:** Accuracy outcomes across the three mediums.

Distance	Medium	Trueness (mm)	Precision (mm)	<i>p</i> -value
$d_1$	<i>air</i>	0.197	0.029	0.264
	<i>glass</i>	0.251	0.004	
	<i>water</i>	0.205	0.271	
$d_2$	<i>air</i>	0.288	0.021	0.717
	<i>glass</i>	0.313	0.069	
	<i>water</i>	0.341	0.430	
$d_3$	<i>air</i>	0.324	0.088	0.264
	<i>glass</i>	0.208	0.131	
	<i>water</i>	0.324	0.380	

The results of the accuracy analysis reveal the highest magnitude of error for the underwater scenario (e.g., the water medium in Table 4-2), which is in line with previous findings [46,59] that suggested these increased errors could be due to light refraction. However, the results in the present study reveal that there is no significant influence from the medium. Hence, there is a potential for using a land-based mo-cap system arranged externally to perform human locomotion analysis in constrained aquatic environments.

Previous findings based on accuracy analyses of land-based mo-cap systems indicate the errors should be estimated in a laboratory or application-specific manner to obtain high-quality research data [14,15]. Following recommendations from these studies, dynamic and static error assessments were performed during an underwater treadmill

exercise with SOLAS reflective markers placed on human subjects at anatomical regions of interest.

The results of this accuracy study offer initial insights to outweigh the minimal threat of inaccuracy in mo-cap for the static error assessments. In agreement with previous findings [46,59], small instrumental errors ( $< 1$  mm) may not seem relevant for biomechanical assessments with large ranges of motion. Hence, this understanding helps quantify the ability and reliability of mo-cap systems in real-time biomechanical assessments of aquatic rehabilitation against conventional pre- and post-assessments [1].

## **4.2 Kinematic Analysis**

### *4.2.1 Influence of the Speed of the Treadmill*

As detailed in section 3.2.3, RMANOVA and Friedman ANOVA determined significant influences of the speed of the treadmill for condition 1 (*air* - treadmill runs without water) and condition 2 (*water* - treadmill runs with water). The outcomes tested are the peak flexion, time to peak flexion, and ROM for the knee as well as the peak DF, time to peak DF, and ROM for the ankle. The RMANOVA results revealed a significant influence of the speed of the treadmill for *air* and *water*. Friedman ANOVA was utilized on the ankle's time to peak flexion for *air* as it was not normally distributed. The results of the kinematic analysis and statistical significances are listed in Table 4-3.



**Table 4-3:** Kinematic parameters (mean  $\pm$  SD) of the gait collected at 1, 2, and 3 mph and the associated results of the statistical analysis to determine the influence of speed for condition 1 and condition 2.

Kinematic parameters	Speed (mph)			<i>p</i> -value	Pairwise comparisons ( <i>p</i> < 0.05)
	1	2	3		
<i>air</i>					
Knee					
Peak flexion (°)	48.14 $\pm$ 7.18	53.32 $\pm$ 5.65	55.16 $\pm$ 5.43	< 0.001	<i>a, b, c</i>
Time to Peak flexion (s)	01.32 $\pm$ 0.14	00.88 $\pm$ 0.06	00.73 $\pm$ 0.04	< 0.001	<i>a, b, c</i>
ROM (°)	47.89 $\pm$ 5.43	52.61 $\pm$ 4.93	53.53 $\pm$ 3.22	< 0.001	<i>a, b</i>
Ankle					
Peak DF (°)	07.71 $\pm$ 3.32	06.81 $\pm$ 3.31	05.07 $\pm$ 3.23	< 0.001	<i>b, c</i>
Time to Peak DF (s)	0.89*	0.60*	0.41*	< 0.001	<i>a, b, c</i>
ROM (°)	21.04 $\pm$ 5.17	25.51 $\pm$ 5.11	27.69 $\pm$ 6.38	0.003	<i>b</i>
<i>water</i>					
Knee					
Peak flexion (°)	49.07 $\pm$ 7.46	53.53 $\pm$ 7.39	57.06 $\pm$ 8.69	0.003	<i>a, b</i>
Time to Peak flexion (s)	01.50 $\pm$ 0.26	01.05 $\pm$ 0.15	00.85 $\pm$ 0.15	< 0.001	<i>a, b, c</i>
ROM (°)	49.53 $\pm$ 7.50	50.81 $\pm$ 8.29	51.33 $\pm$ 8.97	0.702	-
Ankle					
Peak DF (°)	05.71 $\pm$ 3.93	06.01 $\pm$ 4.80	09.76 $\pm$ 7.16	0.016	<i>c</i>
Time to Peak DF (s)	01.01 $\pm$ 0.20	00.83 $\pm$ 0.23	00.61 $\pm$ 0.29	< 0.001	<i>a, b, c</i>
ROM (°)	19.16 $\pm$ 4.02	24.93 $\pm$ 7.70	35.85 $\pm$ 8.93	< 0.001	<i>b, c</i>

\*indicates that the reported value is a median as the data pertaining to 1 mph was not normally distributed. Also, Wilcoxon test was utilized for pairwise comparisons.

Figure 4-1 illustrates the changes in the knee angles in a gait cycle at treadmill speeds of 1, 2, and 3 mph for *air* and *water*. The peak flexion and the ROM for the knee

increase with an increase in the speed of the treadmill for each medium (Figure 4-1A and B). In contrast, the time to peak flexion decreases with an increase in the speed of the treadmill (Table 4-3). This relationship indicates that the time to complete a gait cycle decreases with an increase in the speed of walking, as expected.

Statistically significant differences exist for knee peak flexion ( $F = 29.866$ ,  $df = 1.351$ ,  $p < 0.001$ ), time to peak flexion ( $F = 253.137$ ,  $df = 1.074$ ,  $p < 0.001$ ), and ROM ( $F = 12.103$ ,  $df = 2$ ,  $p < 0.001$ ) at the considered treadmill speeds in *air* (Table 4-3). For the knee angles in *water*, significant differences are observed for peak flexion ( $F = 8.001$ ,  $df = 2$ ,  $p = 0.003$ ) and time to peak flexion ( $F = 112.353$ ,  $df = 1.071$ ,  $p < 0.001$ ) with the increase in the speed of the treadmill. On the other hand, no significant differences are observed for knee ROM ( $F = 0.361$ ,  $df = 2$ ,  $p = 0.702$ ) in *water*.

For the ankle in *air*, the peak ankle DF decreases with an increase in the speed of the treadmill in comparison to an increase in *water* (Figure 4-1C and D). The ankle ROM increases for both *air* and *water* with an increase in the speed of the treadmill (Table 4-3).

Significant differences are observed for peak DF ( $F = 13.801$ ,  $df = 2$ ,  $p < 0.001$ ), time to peak DF ( $df = 2$ ,  $p < 0.001$ ), and ROM ( $F = 7.559$ ,  $df = 2$ ,  $p = 0.003$ ) in *air* (Table 4-3). Additionally, for the ankle in *water* significant differences are observed for peak DF ( $F = 5.207$ ,  $df = 2$ ,  $p = 0.016$ ), time to peak DF ( $F = 19.415$ ,  $df = 2$ ,  $p < 0.001$ ), and ROM ( $F = 29.037$ ,  $df = 2$ ,  $p < 0.001$ ).

The changes in the gait angles with changes in the speed of the treadmill can be ascribed to the need for individuals to walk at the prescribed speeds of the treadmill as



opposed to self-selected speeds. This behavior restricts the available options for the coordination of limb movements, so the gait cycle becomes increasingly constrained [33].

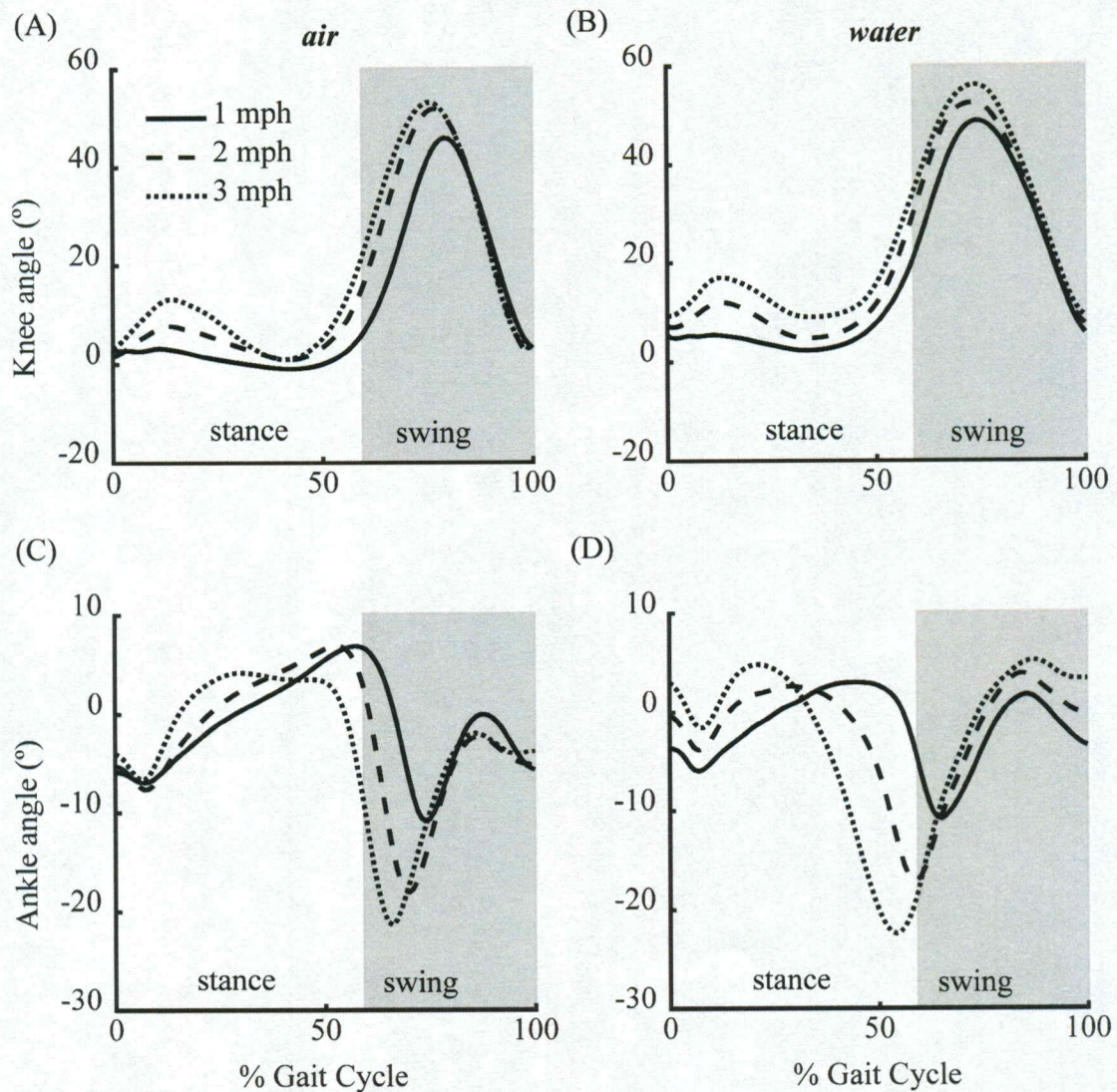


**Figure 4-1:** The mean knee and ankle angles for treadmill speeds of 1 (solid lines), 2 (dashed lines) and 3 (dotted lines) mph. (A) and (B) represent the mean knee angles for condition 1 and condition 2, respectively. (C) and (D) represent the mean ankle angles for condition 1 and condition 2, respectively.

Previously, Jordan *et al.* [33] observed a strong correlation between knee and ankle angles with walking speed for condition 1 (in *air*). They did not consider the second



condition. Their research based these findings on outcomes such as stride length, stride intervals, step length, step intervals, and impulse. The kinematic assessments to ascertain the influence of speed in our study is qualitatively in consensus with this previous finding in terms of variability of gait kinematics with speed.

#### 4.2.2 *Air versus Water Conditions*

As detailed in section 3.2.4, paired sample *t*-tests were used to assess statistically significant differences between walking in *air* and *water*. The corresponding outcomes of kinematic analyses and statistical significances for the two conditions are listed in Table 4-4. Figure 4-2 illustrates the changes in knee and ankle angles in a gait cycle between *air* and *water* at treadmill speeds of 1, 2, and 3 mph.



**Table 4-4:** The mean kinematic parameters of gait collected at 1, 2 and 3 mph and associated results of statistical analyses to determine the influence of the treadmill scenarios of condition 1 versus condition 2.

Kinematic parameters	Speed (mph)	Medium		<i>p</i> -value	Number of subjects ( <i>n</i> )
		<i>air</i>	<i>water</i>		
Knee					
Peak flexion (°)	1	46.78 ± 7.35	49.73 ± 7.28	0.280	12
	2	52.34 ± 6.28	53.71 ± 7.03	0.635	11
	3	54.83 ± 5.26	56.79 ± 8.22	0.448	11
Time to Peak flexion (s)	1	1.31 ± 0.12	1.50 ± 0.25	0.006	12
	2	0.88 ± 0.06	1.06 ± 0.15	0.002	11
	3	0.73 ± 0.04	0.84 ± 0.14	0.010	11
ROM (°)	1	47.57 ± 5.01	49.73 ± 7.44	0.410	12
	2	52.55 ± 4.68	50.69 ± 7.87	0.544	11
	3	53.60 ± 3.07	50.93 ± 8.61	0.330	11
Ankle					
Peak DF (°)	1	8.24 ± 3.31	5.61 ± 3.71	0.033	12
	2	7.09 ± 3.27	6.70 ± 5.10	0.764	11
	3	5.25 ± 3.13	9.07 ± 7.18	0.069	11
Time to Peak DF (s)	1	0.92 ± 0.10	1.07 ± 0.29	0.074	12
	2	0.59 ± 0.08	0.86 ± 0.24	0.003	11
	3	0.39 ± 0.09	0.59 ± 0.29	0.037	11
ROM (°)	1	20.92 ± 4.81	18.85 ± 4.47	0.191	12
	2	24.95 ± 5.19	25.39 ± 7.46	0.861	11
	3	27.64 ± 6.05	34.78 ± 9.19	0.077	11

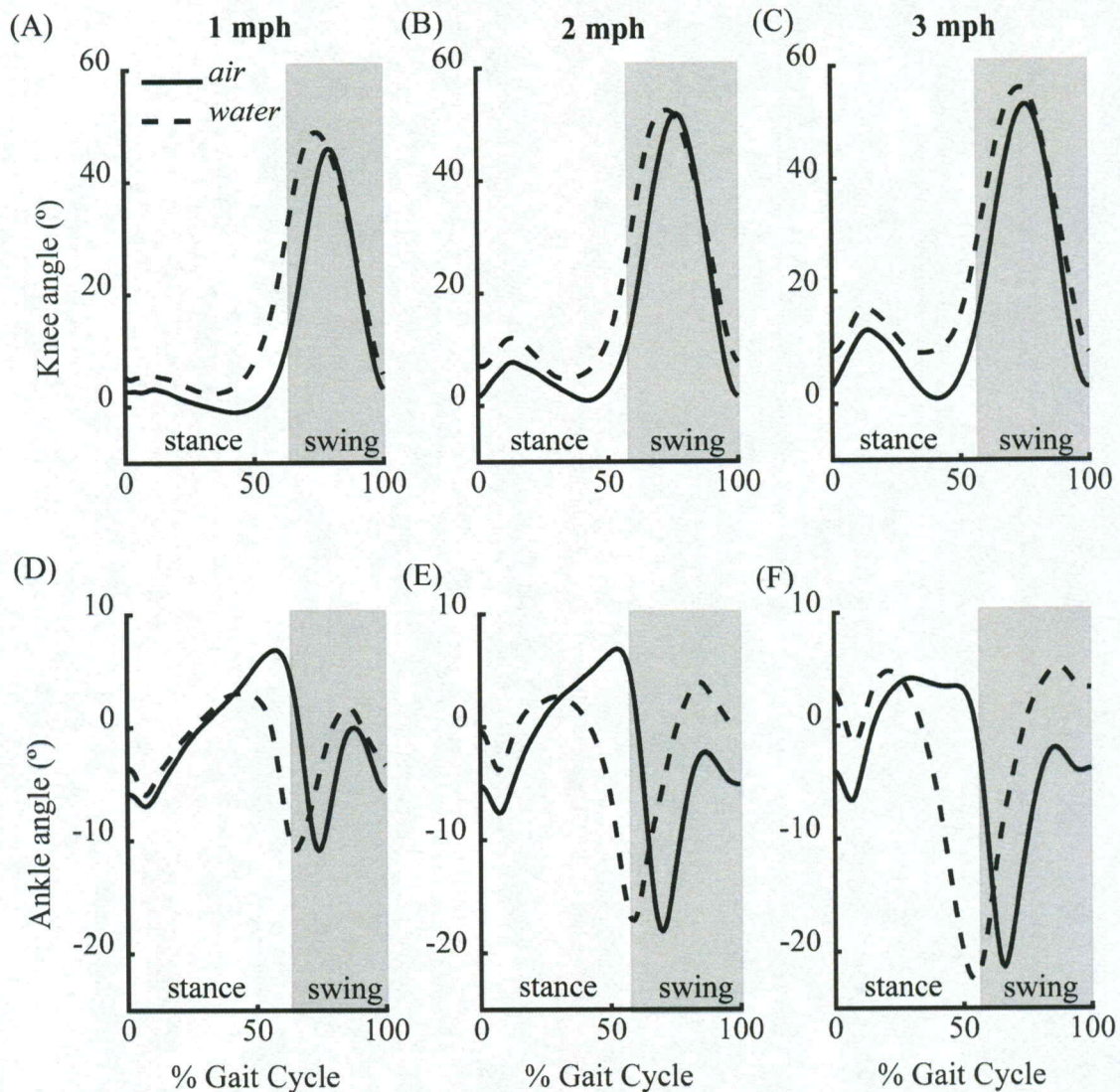


**Figure 4-2:** The variability of the mean knee and ankle angles across a gait cycle in condition 1 (solid black line) and condition 2 (dashed line). (A), (B), and (C) represent the mean knee angles at 1, 2, and 3 mph, respectively, and (D), (E), and (F) represent the mean ankle angles at 1, 2, and 3 mph, respectively.

The knee flexion and extension angles are slightly higher in *water* compared to *air* during the stance phase of the gait cycle for all speeds (Figures 4-2A, B, and C). After the peak flexion is attained, the extension of the knee during the swing phase of the gait cycle in *water* is similar to the extension in *air*. Larger peak flexion values are consistently



observed in *water* compared to *air*. However, this difference is not statistically significant ( $T = -1.135$ ,  $df = 11$ ,  $p = 0.280$  at 1 mph;  $T = -0.490$ ,  $df = 10$ ,  $p = 0.635$  at 2 mph;  $T = -0.790$ ,  $df = 10$ ,  $p = 0.448$  at 3 mph). The ROM for the knee is larger in *water* at 1 mph and smaller at 2 and 3 mph (Table 4-4). However, again, no significant difference is seen between *air* and *water* for the knee ROM ( $T = -0.856$ ,  $df = 11$ ,  $p = 0.410$  at 1 mph;  $T = 0.627$ ,  $df = 10$ ,  $p = 0.544$  at 2 mph;  $T = 1.024$ ,  $df = 10$ ,  $p = 0.330$  at 3 mph). The time to peak flexion is longer in *water* compared to in *air* (Table 4-4). This difference is statistically significant ( $T = -3.398$ ,  $df = 11$ ,  $p = 0.006$  at 1 mph;  $T = -4.304$ ,  $df = 10$ ,  $p = 0.002$  at 2 mph;  $T = -3.182$ ,  $df = 10$ ,  $p = 0.010$  at 3 mph) (Table 4-4).

In contrast to the knee angle, the peak ankle DF is lower in *water* compared to in *air* (Figures 4-2D, E, F) except at a treadmill speed of 3 mph. The peak DF is consistently attained during the early swing phase in *air* as opposed to approximately the mid-stance phase in *water* for the three speeds. Significant differences are observed for the ankle peak DF at 1 mph ( $T = 2.435$ ,  $df = 11$ ,  $p = 0.033$ ). However, no significant differences are observed for the peak DF ( $T = 0.308$ ,  $df = 10$ ,  $p = 0.764$  at 2 mph;  $T = -2.040$ ,  $df = 10$ ,  $p = 0.069$  at 3 mph). The ROM for the ankle in *water* is smaller at 1 mph as opposed to at 2 and 3 mph (Table 4-4). No significant difference is observed for the ankle ROM ( $T = 1.392$ ,  $df = 11$ ,  $p = 0.191$  at 1 mph;  $T = -0.179$ ,  $df = 10$ ,  $p = 0.861$  at 2 mph;  $T = -1.969$ ,  $df = 10$ ,  $p = 0.077$  at 3 mph) between *air* and *water*. Again, the time to peak for the ankle DF is longer in *water* compared to *air* (Table 4-4). No significant difference is observed for the time to peak DF at 1 mph ( $T = -1.975$ ,  $df = 11$ ,  $p = 0.074$ ) between *air* and *water*. However, significant differences exist between the time to peak DF at 2 mph ( $T = -3.970$ ,  $df = 10$ ,  $p = 0.003$ ) and 3 mph ( $T = -2.406$ ,  $df = 10$ ,  $p = 0.037$  at 3 mph) between *air* and *water*.



In summary, the knee and ankle angle amplitude measurements reveal no significant difference between the *air* and *water* ( $p > 0.05$ ) conditions, except for the peak DF of the ankle at 1 mph ( $p < 0.05$ ). In contrast, time outcomes for the knee and ankle kinematics show significant differences between the *air* and *water* ( $p < 0.05$ ) conditions, except for the ankle time to peak DF at 1 mph ( $p > 0.05$ ). These results suggest minimal influences from *water* on the knee and ankle angle magnitudes in comparison to *air*. However, significant differences are observed in the timing of gait outcomes between the *air* and *water* treadmill scenarios (Table 4-4).

The peak knee flexion increases by  $7.0^\circ$  in *air* and  $8.0^\circ$  in *water* when the speed increases from 1 to 3 mph (Table 4-3). The knee ROM for *air* increases by  $5.6^\circ$  as opposed to  $1.2^\circ$  in *water* when the treadmill speed increases from 1 to 3 mph (Table 4-3). These changes indicate that, in *water*, the knee flexion during the initial contact is higher than the knee flexion in *air* (Figures 4-1 and 4-2), thereby reducing the increase in ROM at higher speeds for *water* in comparison to *air*. The increase in peak flexion in *water* is consistent with observations by Jabbar *et al.* [32]. In contrast to the changes in the peak knee flexion, the peak ankle DF for *air* decreases by  $2.6^\circ$  as opposed to an increase of  $4.1^\circ$  in *water* when the speed increases from 1 to 3 mph (Table 4-3). Also, the ankle ROM for *air* increases by  $6.7^\circ$  as opposed to  $16.7^\circ$  in *water* when the speed increases from 1 to 3 mph.

An explanation for the increase in knee ROM in this study, as opposed to the decrease reported by Jabbar *et al.* [32], may stem from the environment of the experiments. Trials in this study were conducted on an aquatic treadmill (1.4 m long  $\times$  0.5 m wide  $\times$  1.3 m deep) whereas Jabbar *et al.* [32] performed trials in a large volume swimming pool (18 m long  $\times$  16 m wide  $\times$  1.2 m deep). In constrained aquatic environments, the fluid dynamic



effects due to sloshing and rebounding may be more significant than those experienced in a larger volume. Nevertheless, further study is warranted to quantify these effects.

Greater time was required to achieve the knee peak flexion and ankle peak DF in *water* than in *air* with an observed average increase of 0.16 seconds for the peak flexion and 0.21 seconds for the peak DF for all speeds in *water*, which is about 20 % of the gait cycle. This extended time requirement in *water* can be explained by the presence of fluid dynamic forces that slow down joint movements and increase the time to achieve control of limb motion [60] as discussed in section 4.3.

The kinematic analysis in *water* reveals two key takeaways. First, increased variability of kinematic outcomes (the knee and ankle angle measures) exists in an aquatic treadmill as opposed to land treadmill walking. Second, significant differences are required in the time taken to achieve peak knee and ankle angles.

### **4.3 Effect of Viscous Drag and Added Mass Forces**

The total fluid dynamic force acting on a body submerged in water is modeled by considering the added mass and viscous drag. As shown in Figure 4-3, the viscous drag per unit length  $F'_d$  opposes the direction of the velocity, whereas the added mass force per unit length  $F'_{\text{added mass}}$  opposes the acceleration.



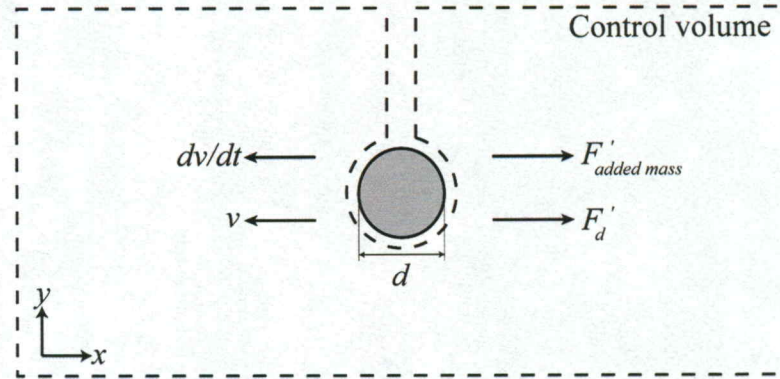


**Figure 4-3:** A control volume showing the directions of the velocity and acceleration of a calf of diameter  $d$  along with the directions of the fluid forces acting on the calf.

We model the calf portion of the leg as a 2-D circular cylinder with diameter  $d = 0.123$  m, as estimated from anthropometric reference data [61], corresponding to the age group 20-29 years to be consistent with the mean age of the participants in this study of  $23.0 \pm 3.6$  years.

Viscous drag per unit length  $F'_d$  is calculated by Eq. 4-1 [63],

$$F'_d = \frac{1}{2} \rho v^2 d C_d, \quad (4-1)$$

where  $\rho$  is the fluid density,  $v$  is velocity,  $d$  is the calf diameter, and  $C_d$  is the drag coefficient. The velocity  $v$  corresponds to the mean velocity of the tibia marker (Figure 3-6), normalized to 101 points per gait cycle from the trajectory information in the lateral direction of motion of the leg for all the participants. The density of air is  $1.23 \text{ kg/m}^3$  at  $59^\circ\text{F}$ , and the density of water is  $994.68 \text{ kg/m}^3$  at  $90^\circ\text{F}$ . The drag coefficient  $C_d$  is estimated from the Reynolds number  $Re$ , which is the ratio of inertial forces to viscous forces as in Eq. 4-2 [63],



$$Re = \frac{\rho v d}{\mu}, \quad (4-2)$$

where  $\mu$  represents the dynamic viscosity of the fluid. For water,  $\mu = 7.61 \times 10^{-4}$  Ns/ m<sup>2</sup> at 90 °F, and for air,  $\mu = 1.79 \times 10^{-4}$  Ns/ m<sup>2</sup>. The values of  $C_d$  are estimated as a function of  $Re$  from the logarithmic graph provided in Figure 4-4 [63].

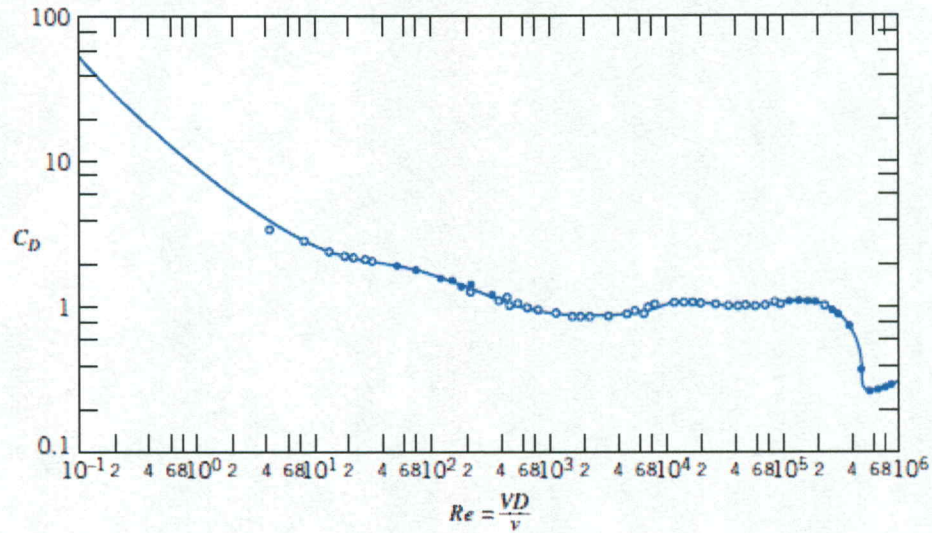


**Figure 4-4:**  $C_d$  vs.  $Re$  for a smooth circular cylinder [63].

Added mass relates to the reactive effect of the fluid on a body due to its acceleration. The force per unit length due to added mass ( $F'_{\text{added mass}}$ ) is calculated by Eq. 4-3 [64],

$$F'_{\text{added mass}} = M'_{11} \frac{dv}{dt}, \quad (4-3)$$

where  $M'_{11}$  represents the added mass coefficient per unit length. The term  $dv/dt$  is the acceleration of the tibia marker normalized to 101 points per gait cycle from the trajectory information in the lateral direction of motion of the leg for all participants. The value of  $M'_{11}$  for a cylinder is calculated by Eq. (4-4) [64], such that

$$M'_{11} = \frac{\pi \rho d^2}{4} = 11.82 \frac{\text{kg}}{\text{m}} \quad (4-4)$$

The total fluid dynamic force is the sum of the viscous drag and added mass force as expressed in Eq. 4-5. Consequently, the power required by the leg to overcome the total fluid dynamic force is calculated by Eq. 4-6.

$$F'_{\text{total}} = F'_d + F'_{\text{added mass}} \quad (4-5)$$

$$\text{Power}_{\text{leg}} = - \text{Power}_{\text{fluid}} = - F'_{\text{total}} v \quad (4-6)$$

Power and mechanical work imply that actual muscle power and muscle work are performed [65]. Positive power and work indicate concentric contractions (i.e., muscle fibers shorten as bony attachments contract) [66] to overcome the fluid dynamic forces acting on the leg [67]. On the other hand, negative power and mechanical work suggest that energy is extracted from the surrounding fluid. Hence, to represent the actual work in air and water, we estimate the positive mechanical work ( $W^+$ ) by numerically integrating the positive power profiles with respect to time at each speed using the trapezoid rule.

Figure 4-5 shows the measured variations of velocity and acceleration of the tibia marker over a gait cycle in air and water. The time history of the velocity showcases a nearly symmetric profile in the stance and swing phases of the gait cycle. Peak velocity magnitudes are observed during mid-stance and mid-swing phases. Peak acceleration magnitudes are observed during the transition from the stance to swing phase. Peak velocity and acceleration magnitudes observed in air are higher than water.



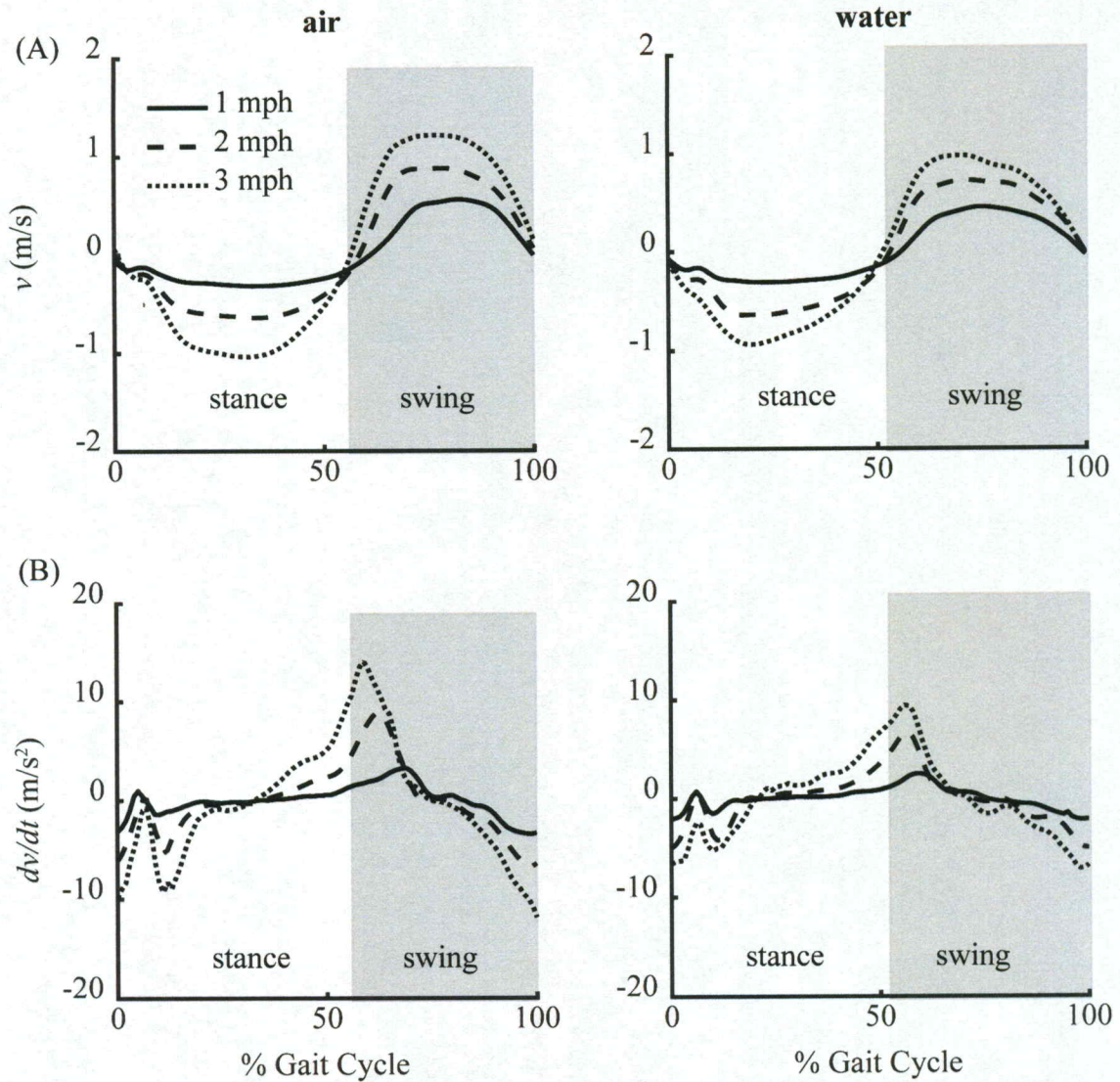


**Figure 4-3:** Velocity and acceleration of the calf modeled as a circular cylinder during a gait cycle.

Figure 4-6 illustrates the variation of  $F'_d$ ,  $F'_{\text{added mass}}$ , and  $F'_{\text{total}}$  over a gait cycle as calculated using Eqs. 4-1, 4-3, and 4-5, respectively. As expected, fluid dynamic forces are about three orders of magnitudes higher in water compared to air because the density of water is 800 times more than that of air.

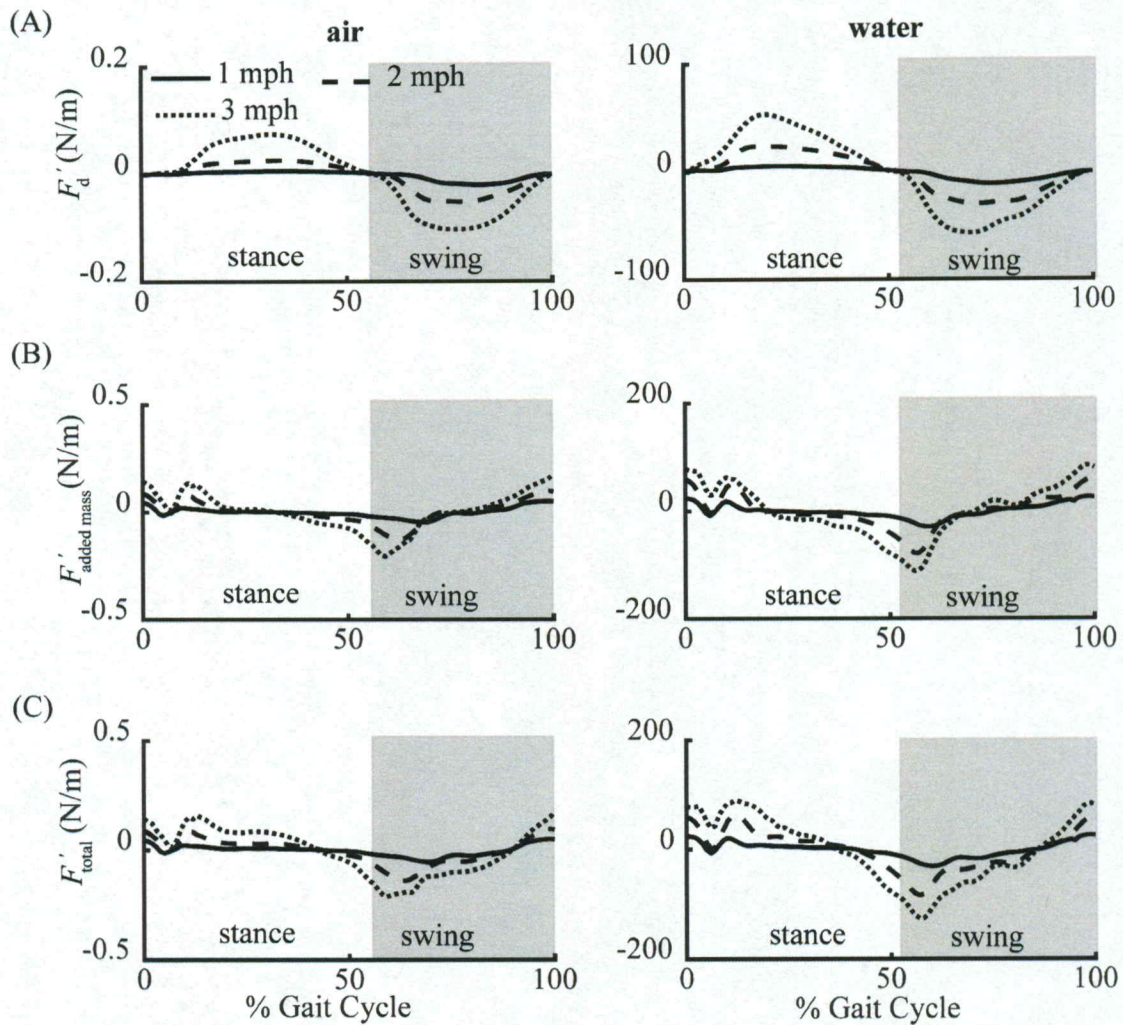


**Figure 4-4:** Estimates of the viscous drag (A), the force due to added mass (B), and total fluid dynamic force (C) over a gait cycle in condition 1 (air) and condition 2 (water).

Viscous drag (Figure 4-6A) has a nearly symmetric profile in the stance and swing phases of the gait in air and water as it is proportional to the square of the velocity. In contrast, the added mass force (Figure 4-6B) is similar to the acceleration profile over the gait cycle as the added mass force is proportional to the acceleration. Maximum viscous drag magnitudes are observed approximately at the mid-stance (between 20-30% of the gait cycle) and the mid-swing phases (between 70-80% of the gait cycle) in air and water. These peak viscous drag magnitudes are also seen during the transition from flexion to



extension of the knee in the stance and swing phases (Figures 4-1A and B). On the other hand, the maximum viscous drag magnitudes are seen during the transition from dorsiflexion to plantarflexion of the ankle in the stance and swing phases (Figures 4-1C and D).

The motion in air and water is also affected by force due to the added mass. Particularly, the magnitude of forces resulting from the added mass is higher in water, which is again due to the higher density of water compared to air. In this study, peak added mass force values in water are observed at the transition from the stance to the swing phase (between 55-65% of the gait cycle). The acceleration is at the highest during the transition from stance to swing in a gait cycle. The greater peaks in the added mass forces are observed at approximately the instance of maximum peak flexion of the knee and maximum planar flexion of the ankle during the transition from the stance to swing phases (Figure 4-1).

The total fluid dynamic force estimates show the presence of higher resistive effects during the beginning and end of the gait cycle as seen in Figure 4-6C, where significant contribution from added mass is observed. Interestingly, in water, significantly higher negative total fluid dynamic force is estimated at speeds of 2 and 3 mph during the swing phase. This suggests that the leg gains significant thrust around the early swing phase in water.

Figure 4-7 illustrates the power required by the leg to overcome the total fluid dynamic force during a gait cycle. The power required is high during the early stance and early swing phases of the gait cycle. The higher magnitude of power required in water



compared to air can be ascribed to the much higher water density that produces orders of magnitude larger fluid dynamic forces in water, whereas the gait is similar (Eq. 4-1). As a consequence, the leg muscles undergo larger muscle contractions in water than in air. This implies that water is a promising exercise medium that can enhance muscle strengthening and training during rehabilitation. Short periods of negative power values are also predicted during the end of the stance and swing phases. This observation suggests that during these phases of gait, the leg muscles undergo eccentric contractions where the muscle extracts energy from the water.

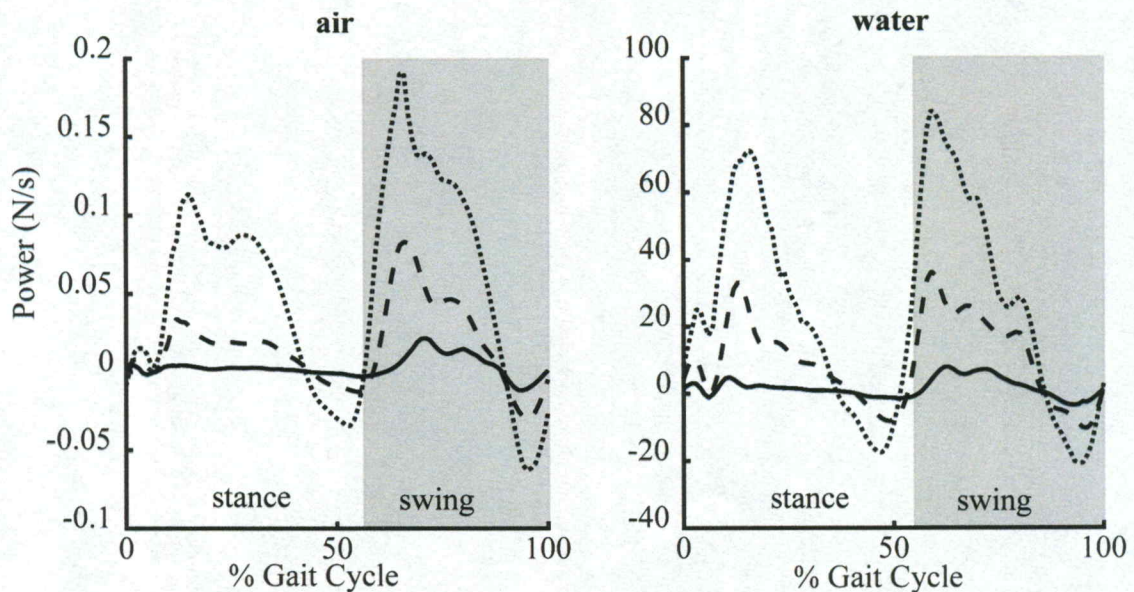


**Figure 4-5:** Power required to overcome the total fluid dynamic force in a gait cycle.

The positive mechanical work done by the leg to overcome the total fluid dynamic force in water is estimated at each speed as listed in Table 4-5, which are significantly larger compared to air. Greater time is required to complete a gait cycle in water than in air. Larger mechanical work is also required at higher speeds that may maximize the benefits of strength training for muscles.



**Table 4-5:** The average time for a gait cycle and the corresponding positive mechanical work.

Speed of treadmill (mph)	Average time of a gait cycle (s)		Positive Mechanical Work ( $W^+$ ) (J/m)	
	air	Water	air	water
1	1.66	2.03	0.01	4.2
2	1.16	1.45	0.02	16.5
3	0.97	1.15	0.06	32.7

During the mid-swing phase, the right and left legs come in close vicinity. While the right leg is in its mid-swing phase, the left is in its stance phase and vice versa. In the mid-swing phase, there is increased fluid activity due to the gait phases of both legs. The resulting flow dynamics are highly nonlinear with unsteady three-dimensional wake structures caused by both legs interacting during their gait cycles. These nonlinear effects, while not modeled in this study, could further increase or decrease the fluid dynamic force magnitudes in water and air. Further study is warranted to ascertain the implications of these nonlinear effects.

## CHAPTER 5

### CONCLUSION AND FUTURE SCOPE

The aquatic rehabilitation using an aquatic treadmill has been under used since its inception due to the challenge of quantifying the effects of water on gait kinematics. This study addresses this challenge by developing the framework to be able to use land-based mo-cap cameras to record lower limb motion in an aquatic treadmill.

The objectives as established in the introduction (Chapter 1) of this research study were as follows:

- To choose marker material capable of preserving the retro-reflective capabilities when submerged.
- To assess the walking kinematics from a biomechanics stand-point, by processing the motion data to obtain gait angles (knee and ankle) in the sagittal plane.
- To quantify the effect of presence of resistive effects due to fluid dynamic forces to analyze the need for larger power and mechanical work to execute a gait cycle in water.



An appropriate material suited for aquatic applications was identified to be SOLAS retro-reflective tape. We evaluated the static accuracy of Vicon T40s mo-cap system in reconstruction of marker distances in water weighed against air and glass. We considered a glass tank setup with and without water to replicate a constrained aquatic environment and evaluated the accuracy outcomes.

The results in terms of accuracy analysis of Vicon T40s mo-cap demonstrated that although water showed higher magnitude of errors than air, statistical analyses revealed that presence of glass and water had no significant influence on the trueness and precision (accuracy outcomes) of the mo-cap cameras. Also, these results revealed there were no significant differences in reconstruction of marker center distances in three mediums: air, glass tank without water, and glass tank with water. Magnitude of instrumental errors being less than 1 mm found in this study outweigh the threat of inaccuracy for biomechanical assessments.

Our results of kinematics analysis revealed that the speed of the treadmill significantly influenced the knee and ankle angles for both water and air trails. Our results indicate that in general there was minimal influence of water on the knee and ankle angles in spite of observing greater peak angle measures in water than on air. This indicates that the gait in water is not different than in air. This finding in this study strengthens clinicians' confidence in suggesting aquatic therapy especially to athletes, who generally prefer not to alter their original gait during rehabilitation.

However, the time measures (time to peak flexion and time to peak DF) showed significant differences between the air and water trials. This indicates that the presence of

larger fluid dynamic forces in water due to the higher density increases the time to complete a gait cycle. From a medical standpoint, this helps in the strengthening of weaker muscles due to the need for limbs to overcome larger resistive effects.

The kinematic information of an aquatic gait reveals promising motivation for aquatic rehabilitation of athletes and treatment for recovery from lower limb injuries. The kinematic information in water in addition to the established understanding of aquatic locomotion from a medical standpoint helps clinicians and athletic trainers to maximize the benefits of aquatic therapy.

## **5.1 Recommendation for Future Research**

As emphasized in the literature survey (Chapter 2), there is a growing body of literature focused on devising methods to decipher locomotion in water. Henceforth, there is a need to further strengthen the interplay between the biomechanical and medical standpoint.

- In this study the gait information is based on healthy college-aged adults with no prior medical conditions. This study can be extended to populations with different medical conditions and older adults to further assess the efficacy of aquatic therapy from a biomechanical standpoint
- The estimates of fluid dynamic forces in this study were based on 2-D cylinder assumption and involved only theoretical estimates. This methodology could further be extended to evaluate fluid dynamic forces using higher fidelity numerical methods such



as the computational fluid dynamic methods. 3-D effects, leg-leg-wake interactions, and detailed body geometric effects need to be quantified.

- This study considered the kinematic information only for the dominant leg of the participants. It can be expected that there could be lesser statistically significant outcomes in the non-dominant gait patterns than dominant gait patterns. However, further study is warranted to understand the interplay between the dominant and non-dominant gait pattern and their relevance to aquatic therapy.
- The approach in this study can be used in other scientific and engineering communities. For example, capturing the motion of autonomous underwater vehicles can greatly benefit from our proposed approach to capture aquatic locomotion
- Dynamic accuracy of mo-cap systems can be evaluated using similar approach in aquatic medium. However, dynamic accuracy study warrants a robotic framework that could produce a repeatable motion.
- There is a need to quantify the correlation between different parameters, such as the height of cameras, size of the capture volume, number of cameras, and depth of the water and the thickness of the glass interface.

## **5.2 Novel Contributions**

- The ability of Vicon T40s motion capture was advanced to reconstruct markers in aquatic environments
- Biomechanical assessments were made after understanding the accuracy implications of land-based mo-cap systems in aquatic environment. Therefore, a methodological

framework was developed for land-based mo-cap systems to understand the locomotion in water systematically.



**APPENDIX A**

IRB Approval



July 12<sup>th</sup> 2018

Shreyas L. Raghu

Department of Kinesiology

University of Alabama in Huntsville

<input checked="" type="checkbox"/> Expedited (see pg 2)
<input type="checkbox"/> Exempted (see pg 3)
<input type="checkbox"/> Full Review
<input type="checkbox"/> Extension of Approval

Dear Mrs. Raghu,

The UAH Institutional Review Board of Human Subjects Committee has reviewed your proposal, *Kinematics Study, Computational Fluid Dynamics (CFD) Simulation and Evaluation of Biomechanics of Human Locomotion in an Underwater Treadmill*, and found it meets the necessary criteria for approval. Your proposal seems to be in compliance with this institutions Federal Wide Assurance (FWA) 00019998 and the DHHS Regulations for the Protection of Human Subjects (45 CFR 46).

Please note that this approval is good for one year from the date on this letter. If data collection continues past this period, you are responsible for processing a renewal application a minimum of 60 days prior to the expiration date.

No changes are to be made to the approved protocol without prior review and approval from the UAH IRB. All changes (e.g. a change in procedure, number of subjects, personnel, study locations, new recruitment materials, study instruments, etc) must be prospectively reviewed and approved by the IRB before they are implemented. You should report any unanticipated problems involving risks to the participants or others to the IRB Chair.

If you have any questions regarding the IRB's decision, please contact me.

Sincerely,

A handwritten signature in black ink that reads "Bruce Stallsmith". The signature is written in a cursive style with a large, prominent initial "B".

Bruce Stallsmith

IRB Chair

Professor, Biological Sciences



## **Expedited:**

] Clinical studies of drugs and medical devices only when condition (a) or (b) is met. (a) Research on drugs for which investigational new drug application (21 CFR Part 312) is not required. (Note: Research on marketed drugs that significantly increases the risks or decreases the acceptability of the risks associated with the use of the product is not eligible for expedited review. (b) Research on medical devices for which (i) an investigational device exemption application (21 CFR Part 812) is not required; or (ii) the medical device is cleared/approved for marketing and the medical device is being used in accordance with its cleared/approved labeling.

] Collection of blood samples by finger stick, heel stick, ear stick, or venipuncture as follows: (a) from healthy, nonpregnant adults who weigh at least 110 pounds. For these subjects, the amounts drawn may not exceed 550 ml in an 8 week period and collection may not occur more frequently than 2 times per week; or (b) from other adults and children. Considering the age, weight, and health of the subjects, the collection procedure, the amount of blood to be collected, and the frequency with which it will be collected. For these subjects, the amount drawn may not exceed the lesser of 50 ml or 3 ml per kg in an 8 week period and collection may not occur more frequently than 2 times per week.

] Prospective collection of biological specimens for research purposes by noninvasive means. Examples: (a) hair and nail clippings in a nondisfiguring manner; (b) deciduous teeth at time of exfoliation or if routine patient care indicates a need for extraction; (c) permanent teeth if routine patient care indicates a need for extraction; (d) excreta and external secretions (including sweat); (e) uncannulated saliva collected either in an unstimulated fashion or stimulated by chewing on a base or wax or by applying a dilute citric solution to the tongue; (f) placenta removed at delivery; (g) amniotic fluid retained at the time of rupture of the membrane prior to or during labor; (h) supra- and subgingival dental plaque and calculus, provided the collection procedure is not more invasive than routine prophylactic scaling of the teeth and the process is accomplished in accordance with accepted prophylactic techniques; (i) mucosal and skin cells collected by nasal scraping or swab, skin swab, or mouth washings; (j) sputum collected after saline mist nebulization.

] Collection of data through noninvasive procedures (not involving general anesthesia or sedation) routinely employed in clinical practice, excluding procedures involving x-rays or microwaves. Where medical devices are employed, they must be cleared/approved for marketing. (Studies intended to evaluate the safety and effectiveness of the medical device are not generally eligible for expedited review, including studies of cleared medical devices for new indications).

] Research involving materials (data, documents, records, or specimens) that have been collected, or will be collected solely for nonresearch purposes (such as medical treatment or diagnosis).

] Collection of data from voice, video, digital, or image recordings made for research purposes.

] Research on individual or group characteristics or behavior (including, but not limited to, research on perception, cognition, motivation, identity, language, communication, cultural beliefs or practices, and social behavior) or research employing survey, interview, oral history, focus group, program evaluation, human factors evaluation, or quality assurance methodologies.



## Exempt

Research conducted in established or commonly accepted educational settings, involving normal educational practices, such as (a) research on regular and special education instructional strategies, or (b) research on the effectiveness of or the comparison among instructional techniques, curricula, or classroom management methods. The research is not FDA regulated and does not involve prisoners as participants.

Research involving the use of educational tests (cognitive, diagnostic, aptitude, achievement), survey procedures, interviews, or observation of public behavior in which information is obtained in a manner that human subjects cannot be identified directly or through identifiers linked to the subjects and any disclosure of the human subject's responses outside the research would NOT place the subjects at risk of criminal or civil liability or be damaging to the subject's financial standing, employability, or reputation. The research is not FDA regulated and does not involve prisoners as participants.

Research involving the use of educational tests (cognitive, diagnostic, aptitude, achievement) survey procedures, interview procedures, or observation of public behavior if (a) the human subjects are elected or appointed public officials or candidates for public office, or (b) Federal statute(s) require(s) without exception that the confidentiality of the personally identifiable information will be maintained throughout the research and thereafter. The research is not FDA regulated and does not involve prisoners as participants.

Research involving the collection or study of existing data, documents, records, pathological specimens, or diagnostic specimens, if these sources are publicly available or if the information is recorded by the investigator in such a manner that subjects cannot be identified, directly or through identifiers linked to the subjects. The research is not FDA regulated and does not involve prisoners as participants.

Research and demonstration projects which are conducted by or subject to the approval of department or agency heads, and which are designed to study, evaluate, or otherwise examine: (i) public benefit or service programs; (ii) procedures for obtaining benefits or services under those programs; (iii) possible changes in or alternatives to those programs or procedures; or (iv) possible changes in methods or levels of payment for benefits or services under those programs. The protocol will be conducted pursuant to specific federal statutory authority; has no statutory requirement for IRB review; does not involve significant physical invasions or intrusions upon the privacy interests of the participant; has authorization or concurrent by the funding agency and does not involve prisoners as participants.

Taste and food quality evaluation and consumer acceptance studies, (i) if wholesome foods without additives are consumed or (ii) if a food is consumed that contains a food ingredient at or below the level and for a use found to be safe, or agricultural chemical or environmental contaminant at or below the level found to be safe, by the Food and



Drug Administration or approved by the Environmental Protection Agency or the Food Safety and Inspection Service of the U.S. Department of Agriculture. The research does not involve prisoners as participants.

1 Surveys, interviews, or observation of public behavior involving children cannot be exempt.

## APPENDIX B

### TABLE OF PEAK KINEMATIC ANGLES

**Table B-1:** Mean kinematic angles and time measures for knee and ankle joints.

Condition 1						
Participant	Peak knee flexion (°)	Time to peak knee flexion (secs)	Peak DF (°)	Time to peak DF (s)	Knee ROM (°)	Ankle ROM (°)
1 mph						
1	42.72	1.29	10.27	1	57.44	22.88
2	36.22	1.52	4.99	1.18	39.05	16.19
3	36.88	1.33	9.53	0.97	47.43	17.79
5	49.17	1.21	7.1	0.87	48.67	15.74
6	43.72	1.15	5.04	0.88	46.88	17.65
7	43.08	1.27	12.34	0.91	44.5	22.93
8	43.87	1.23	6.58	0.83	46.39	15.46
9	46.8	1.38	14.76	0.87	42.9	20.13
10	60.96	1.44	4.46	0.95	49.03	24.71
11	56.65	1.42	4.74	0.89	54.96	30.89
12	51.66	1.44	8.94	0.89	49.44	26.57
13	49.61	1.13	10.19	0.84	44.16	20.14
2 mph						



1	50.47	0.94	9.07	0.67	61.45	32.59
2	43.9	0.91	7.52	0.65	46	18.46
3	42.49	0.93	9.95	0.68	51.91	19.39
5	52.56	0.85	6.3	0.58	51.15	18.02
6	52.31	0.85	3.39	0.61	54.85	27.3
7	49.77	0.91	10.65	0.63	51.76	31.18
8	54.66	0.9	6.23	0.59	55.1	27.81
9	53.14	0.89	13.34	0.59	49.85	26.53
10	66.43	0.95	4.86	0.65	56.47	28.61
11	53.92	0.77	1.26	0.42	53.15	19.6
12	50.21	0.92	7.86	0.57	44.85	30.49
13	55.63	0.82	8.22	0.48	53.24	25.69

3 mph

1	49.62	0.75	4.07	0.42	54.93	35.19
2	47.17	0.78	5.29	0.49	49.11	19.32
3	41.65	0.74	6.98	0.57	47.58	18.08
5	52.99	0.7	2.5	0.4	51.46	19.09
6	53.65	0.72	0.68	0.39	54.58	24.2
7	51.55	0.71	7.03	0.41	54.34	27.07
8	57.9	0.73	5.95	0.36	57.3	24.21
9	53.03	0.74	9.87	0.44	51.3	29.53
10	66.92	0.79	3.41	0.49	58.13	25.85
11	57.65	0.66	1.44	0.23	54.79	28.03

12	54.88	0.78	9.23	0.39	48.76	34.23
13	57.77	0.68	8.27	0.23	54.91	37.29
<b>Condition 2</b>						
Participant	Peak knee flexion (°)	Time to peak knee flexion (secs)	Peak DF (°)	Time to peak DF (s)	Knee ROM (°)	Ankle ROM (°)
1 mph						
1	41.49	1.17	9.46	0.9	47.54	17.92
2	48.61	1.69	10.59	1.39	38.14	16.83
3	58.28	1.74	7.55	1.78	57.81	23.19
5	48.25	1.3	4.14	0.9	48.31	15.65
6	49.68	1.31	3.21	1.19	51.85	17.18
7	47.76	1.26	2.62	0.93	43.66	11.48
8	36.44	1.33	4.82	0.82	43.62	14.97
9	60.27	1.86	11.33	1.07	66.65	25.42
10	59.74	1.75	1.1	0.97	53.53	18.55
11	49.5	1.41	1.21	1.16	47.31	21.95
12	52.96	1.84	8.63	0.97	52.06	26.34
13	43.77	1.36	2.6	0.72	46.24	16.77
2 mph						
1	47.79	0.85	7.65	0.54	46.31	15.86
2	55.01	1.06	11.05	0.97	41.56	20.34
3	55.53	1.15	13.64	1.18	49.54	29.99



5	47.65	0.95	-0.11	0.8	48.65	17.55
6	61.21	1.14	11.49	1.07	61.07	38.27
7						
8	42	0.95	3.41	0.77	47.61	19.92
9	65.04	1.25	11.03	1.06	65.53	23.64
10	59.63	1.26	3.78	0.86	52.37	29.63
11	50.42	0.96	-1.83	0.85	43.29	24.56
12	58.27	1.22	9.24	1.02	58.47	36.9
13	48.27	0.89	4.39	0.36	43.19	22.66

---

3 mph

---

1	43.68	0.66	7.5	0.32	39.04	21.25
2	63.96	0.88	17.26	0.81	47.86	39.02
3						
5	47.57	0.75	-1.49	0.88	48.97	25.56
6	61.9	0.99	10.89	1.17	63.91	49.68
7	54.05	0.81	2.09	0.37	46.91	24.02
8	59.73	0.83	5.56	0.35	60.57	35.35
9	66.37	0.98	21.56	0.55	59.96	41.52
10	68.81	1.05	12.78	0.64	58.61	43.43
11	47.68	0.78	1.18	0.61	39.55	31.56
12	56.5	0.94	12.13	0.46	50.15	42.26
13	54.44	0.62	11.56	0.21	44.71	28.9

---

## REFERENCES

- [1] Denning, W. E., Bressel, E., and Dolny, D. G., "Underwater Treadmill Exercise as a Potential Treatment for Adults with Osteoarthritis," *International Journal of Aquatic Research and Education*, vol. 4, 2010, pp. 70-80.
- [2] Conners, R. T., Morgan, D. W., Fuller, D. K., and Caputo, J. L., "Underwater Treadmill Training, Glycemic Control, and Health-Related Fitness in Adults with Type 2 Diabetes," *International Journal of Aquatic Research and Education*, vol. 8, 2014, pp. 382–396.
- [3] Conners, R. T., Caputo, J. L., Coons, J. M., Fuller, D. K., and Morgan, D. W., "Impact of Underwater Treadmill Training on Glycemic Control, Blood Lipids, and Health-Related Fitness in Adults with Type 2 Diabetes," *Clinical Diabetes*, vol. 8, 2018, pp. 36-43.
- [4] Hinman, R. S., Heywood, S. E., and Day, A. R., "Aquatic Physical Therapy for Hip and Knee Osteoarthritis: Results of a Single-Blind Randomized Controlled Trial," *Physical Therapy*, vol. 87, 2007, pp. 32–43.
- [5] Becker, B. E., "Aquatic Therapy: Scientific Foundations and Clinical Rehabilitation Applications," *PM and R*, vol. 1, 2009, pp. 859–872.
- [6] Kwon, Y., and Casebolt, J. B., "Effects of Light Refraction on the Accuracy of Camera Calibration and Reconstruction in Underwater Motion Analysis," *Sports Biomechanics*, vol. 5, 2006, pp. 315–340.
- [7] Silvatti, A. P., Cerveri, P., Telles, T., Dias, F. A. S., Baroni, G., and Barros, R. M. L., "Quantitative Underwater 3D Motion analysis using Submerged Video Cameras: Accuracy Analysis and Trajectory Reconstruction," *Computer Methods in Biomechanics and Biomedical Engineering*, vol. 16, 2013, pp. 1240–1248.
- [8] Muller, A., Germain, C., Pontonnier, C., and Dumont, G., "A Simple Method to Calibrate Kinematical Invariants: Application to Overhead Throwing," *International Society of Biomechanics in Sports*, 2015, pp. 2–5.
- [9] Thewlis, D., Bishop, C., Daniell, N., and Paul, G., "Next-Generation Low-Cost Motion Capture Systems Can Provide Comparable Spatial Accuracy to High-End Systems," *Journal of Applied Biomechanics*, vol. 29, 2013, pp. 112–117.



- [10] Andriacchi, T. P., and Alexander, E. J., “Studies of Human Locomotion: past, present and future,” *Journal of Biomechanics*, vol. 33, 2000, pp. 1217–1224.
- [11] Richards, J. G., “The Measurement of Human Motion: A Comparison of Commercially Available Systems,” *Human Movement Science*, vol. 18, 1999, pp. 589–602.
- [12] Kaufman, K., Miller, E., Kingsbury, T., Russell Esposito, E., Wolf, E., Wilken, J., and Wyatt, M., “Reliability of 3D Gait Data across Multiple Laboratories,” *Gait and Posture*, vol. 49, 2016, pp. 375–381.
- [13] Miller, E., Kaufman, K., Kingsbury, T., Wolf, E., Wilken, J., and Wyatt, M., “Mechanical Testing for Three-Dimensional Motion Analysis Reliability,” *Gait and Posture*, vol. 50, 2016, pp. 116–119.
- [14] Eichelberger, P., Ferraro, M., Minder, U., Denton, T., Blasimann, A., Krause, F., and Baur, H., “Analysis of Accuracy in Optical Motion Capture – A Protocol for Laboratory Setup Evaluation,” *Journal of Biomechanics*, vol. 49, 2016, pp. 2085–2088.
- [15] Windolf, M., Götzen, N., and Morlock, M., “Systematic Accuracy and Precision Analysis of Video Motion Capturing Systems - Exemplified on the Vicon-460 System,” *Journal of Biomechanics*, vol. 41, Aug. 2008, pp. 2776–2780.
- [16] Bregler, C., “Motion Capture Technology for Entertainment,” *IEEE Signal Processing Magazine*, vol. 24, 2007, pp. 160–158.
- [17] Sutherland, D. ., “The Evolution of Clinical Gait Analysis,” *Gait & Posture*, vol. 16, 2002, pp. 159–179.
- [18] Bini, R. R., Diefenthaler, F., and Mota, C. B., “Fatigue Effects on the Coordinative Pattern during Cycling: Kinetics and Kinematics Evaluation,” *Journal of Electromyography and Kinesiology*, vol. 20, 2010, pp. 102–107.
- [19] Marey, E.-J., *Animal Mechanism: A Treatise on Terrestrial and Aerial locomotion*, New York: D. Appleton and Company, 1874.
- [20] Muybridge, E., *Animal locomotion*, Philadelphia: University of Pennsylvania, 1887.
- [21] Karatsidis, A., *Kinetic Gait Analysis using Inertial Motion Capture : New Tools for Knee Osteoarthritis*, Enschede, The Netherlands: 2018.
- [22] Kirk, A. G., O’Brien, J. F., and Forsyth, D. A., “Skeletal Parameter Estimation from Optical Motion Capture Data,” *Computer Society Conference on Computer Vision and Pattern Recognition*, IEEE, 2005, pp. 782–788.



- [23] Roetenberg, D., Luinge, H., and Slycke, P., "Xsens MVN : Full 6DOF Human Motion Tracking Using Miniature Inertial Sensors", *Xsens Motion Technologies BV*, Technical Report 1, 2009.
- [24] Cloete, T., "Clinical Gait Analysis," *Encyclopedia of Neuroscience*, Berlin, Heidelberg: Springer Berlin Heidelberg, 2008, pp. 750–751.
- [25] Aurand, A. M., Dufour, J. S., and Marras, W. S., "Accuracy Map of an Optical Motion Capture System with 42 or 21 Cameras in a Large Measurement Volume," *Journal of Biomechanics*, vol. 58, 2017, pp. 237–240.
- [26] Lu, T.-W., and Chang, C.-F., "Biomechanics of human movement and its clinical applications," *The Kaohsiung Journal of Medical Sciences*, vol. 28, 2012, pp. S13–S25.
- [27] "Planes of Body" Available:  
[https://commons.wikimedia.org/wiki/File:Planes\\_of\\_Body.jpg](https://commons.wikimedia.org/wiki/File:Planes_of_Body.jpg).
- [28] Wikipedia contributors, "Gait analysis - Wikipedia, The Free Encyclopedia" Available:  
[https://en.wikipedia.org/w/index.php?title=Gait\\_analysis&oldid=893652757](https://en.wikipedia.org/w/index.php?title=Gait_analysis&oldid=893652757).
- [29] Frankel, V. H., Forssén, K., Nachamie, H., and Yelle, L., *Basic Biomechanics of the Musculoskeletal System*, Philadelphia: Lea & Febiger, 1989.
- [30] Vishnoi, N., Duric, Z., and Gerber, N. L., "Markerless Identification of Key Events in Gait Cycle using Image Flow," *Proceedings of the Annual International Conference of the IEEE Engineering in Medicine and Biology Society*, 2012, pp. 4839–4842.
- [31] Russell Esposito, E., Stinner, D. J., Ferguson, J. R., and Wilken, J. M., "Gait Biomechanics following Lower Extremity Trauma: Amputation vs. Reconstruction," *Gait and Posture*, vol. 54, 2017, pp. 167–173.
- [32] Abdul Jabbar, K., Kudo, S., Goh, K. W., and Goh, M. R., "Comparison in Three Dimensional Gait Kinematics between Young and Older Adults on Land and in Shallow Water," *Gait and Posture*, vol. 57, 2017, pp. 102–108.
- [33] Jordan, K., Challis, J. H., and Newell, K. M., "Walking Speed Influences on Gait Cycle Variability," *Gait and Posture*, vol. 26, 2007, pp. 128–134.
- [34] Rendos, N. K., Harrison, B. C., Dicharry, J. M., Sauer, L. D., and Hart, J. M., "Sagittal Plane Kinematics during the Transition Run in Triathletes," *Journal of Science and Medicine in Sport*, vol. 16, 2013, pp. 259–265.



- [35] Umberger, B. R., “Stance and Swing Phase Costs in Human Walking,” *Journal of The Royal Society Interface*, vol. 7, 2010, pp. 1329–1340.
- [36] Masumoto, K., and Mercer, J. A., “Biomechanics of Human Locomotion in Water,” *Exercise and Sport Sciences Reviews*, vol. 36, 2008, pp. 160–169.
- [37] Masumoto, K., Takasugi, S., Hotta, N., Fujishima, K., and Iwamoto, Y., “Muscle Activity and Heart Rate Response during Backward Walking in Water and on Dry Land,” *European Journal of Applied Physiology*, vol. 94, 2005, pp. 54–61.
- [38] Masumoto, K., Takasugi, S., Hotta, N., Fujishima, K., and Iwamoto, Y., “Electromyographic Analysis of Walking in Water in Healthy Humans,” *Journal of Physiological Anthropology and Applied Human Science*, vol. 23, 2004, pp. 119–127.
- [39] Fujishima, K., and Shimizu, T., “Body Temperature, Oxygen Uptake and Heart Rate during Walking in Water and on Land at an Exercise Intensity Based on RPE in Elderly Men,” *Journal of Physiological Anthropology and Applied Human Science*, vol. 22, 2003, pp. 83–88.
- [40] Oda, S., Matsumoto, T., Nakagawa, K., and Moriya, K., “Relaxation Effects in Humans of Underwater Exercise of Moderate Intensity,” *European Journal of Applied Physiology and Occupational Physiology*, vol. 80, 1999, pp. 253–259.
- [41] Hall, J., Macdonald, I. A., Maddison, P. J., and O’Hare, J. P., “Cardiorespiratory Responses to Underwater Treadmill Walking in Healthy Females,” *European Journal of Applied Physiology*, vol. 77, 1998, pp. 278–284.
- [42] Shono, T., Fujishima, K., Hotta, N., Ogaki, T., and Masumoto, K., “Cardiorespiratory Response to Low-Intensity Walking in Water and on Land in Elderly Women,” *Journal of Physiological Anthropology and Applied Human Science*, vol. 20, 2004, pp. 269–274.
- [43] Boudarham, J., Roche, N., Pradon, D., Bonnyaud, C., Bensmail, D., and Zory, R., “Variations in Kinematics during Clinical Gait Analysis in Stroke Patients,” *PLoS ONE*, vol. 8, 2013.
- [44] Kang, H. G., and Dingwell, J. B., “Effects of Walking speed, Strength and Range of Motion on Gait Stability in Healthy Older Adults,” *Journal of Biomechanics*, vol. 41, 2008, pp. 2899–2905.
- [45] Barela, A. M. F., Stolf, S. F., and Duarte, M., “Biomechanical Characteristics of Adults Walking in Shallow Water and on Land,” *Journal of Electromyography and Kinesiology*, vol. 16, 2006, pp. 250–256.
- [46] Lauder, M. A., Dabnichki, P., and Bartlett, R. M., “Three-Dimensional



- Reconstruction Accuracy within a Calibrated Volume,” *Proceedings of 2nd International Conference on the Engineering of Sport*, S. Haake, ed., 1998, pp. 441–448.
- [47] Zimmerman, D. W., and Zumbo, B. D., “Relative Power of the Wilcoxon Test, the Friedman Test, and Repeated-Measures ANOVA on Ranks,” *The Journal of Experimental Education*, vol. 62, 1993, pp. 75–86.
- [48] Herda, L., Fua, P., Plänklers, R., Boulic, R., and Thalmann, D., “Using Skeleton-Based Tracking to Increase the Reliability of Optical Motion Capture,” *Human Movement Science*, vol. 20, 2001, pp. 313–341.
- [49] Woltring, H. J., “A Fortran Package for Generalized, Cross-Validatory Spline Smoothing and Differentiation,” *Advances in Engineering Software (1978)*, vol. 8, 1986, pp. 104–113.
- [50] Cappaert, J. M., Pease, D. L., and Troup, J. P., “Three-Dimensional Analysis of the Men’s 100-m Freestyle during the 1992 Olympic Games,” *Journal of Applied Biomechanics*, vol. 11, 1995, pp. 103–112.
- [51] Gourgoulis, V., Aggeloussis, N., Vezos, N., Kasimatis, P., Antoniou, P., and Mavromatis, G., “Estimation of Hand Forces and Propelling Efficiency during Front Crawl Swimming with Hand Paddles,” *Journal of Biomechanics*, vol. 41, 2008, pp. 208–215.
- [52] Maynard, V., Bakheit, A. M. O., Oldham, J., and Freeman, J., “Intra-Rater and Inter-Rater Reliability of Gait Measurements with CODA mpx30 Motion Analysis system,” *Gait and Posture*, vol. 17, 2003, pp. 59–67.
- [53] Zeni, J. A., Richards, J. G., and Higginson, J. S., “Two Simple Methods for Determining Gait Events during Treadmill and Overground Walking using Kinematic Data,” *Gait and Posture*, vol. 27, 2008, pp. 710–714.
- [54] “Knee and ankle angles” Available: <https://basicmedicalkey.com/lower-limb-2/%0A>.
- [55] van Melick, N., Meddeler, B. M., Hoozeboom, T. J., Nijhuis-van der Sanden, M. W. G., and van Cingel, R. E. H., “How to Determine Leg Dominance: The Agreement between Self-Reported and Observed Performance in Healthy Adults,” *PLOS ONE*, vol. 12, 2017, p. e0189876.
- [56] Johanson, M. A., Cooksey, A., Hillier, C., Kobbeman, H., and Stambaugh, A., “Heel Lifts and the Stance Phase of Gait in Subjects with Limited Ankle Dorsiflexion,” *Journal of athletic training*, vol. 41, 2006, pp. 159–65.
- [57] Field, A., *Discovering Statistics Using SPSS*, California: 2009.



- [58] Libraries, K. S. U., "SPSS tutorials: Independent Samples t Test" Available: <https://libguides.library.kent.edu/SPSS/citation>.
- [59] Gourgoulis, V., Aggeloussis, N., Kasimatis, P., Vezos, N., Boli, A., and Mavromatis, G., "Reconstruction Accuracy in Underwater Three-Dimensional Kinematic Analysis," *Journal of Science and Medicine in Sport*, vol. 11, 2008, pp. 90–95.
- [60] Douris, P., Southard, V., Varga, C., Schauss, W., Gennaro, C., and Reiss, A., "The Effect of Land and Aquatic Exercise on Balance Scores in Older Adults," *Journal of Geriatric Physical Therapy*, vol. 26, 2003, pp. 3–6.
- [61] McDowell, M. A., Fryar, C. D., Ogden, C. L., and Flegal, K. M., "Anthropometric Reference Data for Children and Adults: United States, 2003–2006.," *National health statistics reports*, 2008, pp. 1–48.
- [62] Pöyhönen, T., Keskinen, K. L., Hautala, A., and Mälkiä, E., "Determination of Hydrodynamic Drag Forces and Drag Coefficients on Human Leg/Foot Model during Knee Exercise," *Clinical Biomechanics*, vol. 15, 2000, pp. 256–260.
- [63] Fox, R. W., McDonald, A. T., and Pitchard, P. J., *Introduction to Fluid Mechanics*, New Jersey: John Wiley & Sons, Inc, 2006.
- [64] C.E.Brennen, *A Review of Added Mass and Fluid Inertial Forces*, California: Naval Civil Engineering Laboratory, 1982.
- [65] Farris, D. J., and Sawicki, G. S., "The Mechanics and Energetics of Human Walking and Running," vol. 9, 2012, pp. 110–118.
- [66] Newham, D. J., McPhail, G., Mills, K. R., and Edwards, R. H. T., "Ultrastructural Changes after Concentric and Eccentric Contractions of Human Muscle," *Journal of the Neurological Sciences*, vol. 61, 1983, pp. 109–122.
- [67] Knuttgen, H. G., and Kraemer, W. J., "Terminology and Measurement in Exercise Performance," *Journal of Applied Sport Science Research*, vol. 1, 1987, pp. 1–10.
- [68] Killgore, G. L., Wilcox, A. R., Caster, B. L., and Wood, T. M., "A Lower-Extremities Kinematic Comparison of Deep-Water Running Styles and Treadmill Running," *Journal of Strength and Conditioning Research*, vol. 20, 2006, pp. 919–927.